

SMAI-JCM
SMAI JOURNAL OF
COMPUTATIONAL MATHEMATICS

A fully-mixed finite element method
for the steady state
Oberbeck–Boussinesq system

ELIGIO COLMENARES, GABRIEL N. GATICA,
SEBASTIÁN MORAGA & RICARDO RUIZ-BAIER

Volume 6 (2020), p. 125-157.

<http://smai-jcm.centre-mersenne.org/item?id=SMAI-JCM_2020__6__125_0>

© Société de Mathématiques Appliquées et Industrielles, 2020

Certains droits réservés.



Publication membre du

Centre Mersenne pour l'édition scientifique ouverte

<http://www.centre-mersenne.org/>

Sousmission sur <https://smai-jcm.math.cnrs.fr/index.php/SMAI-JCM>





A fully-mixed finite element method for the steady state Oberbeck–Boussinesq system

ELIGIO COLMENARES¹
GABRIEL N. GATICA²
SEBASTIÁN MORAGA³
RICARDO RUIZ-BAIER⁴

¹ Departamento de Ciencias Básicas, Facultad de Ciencias, Universidad del Bío-Bío, Campus Fernando May, Chillán, Chile.

E-mail address: ecolmenares@ubiobio.cl

² CI²MA and Departamento de Ingeniería Matemática, Universidad de Concepción, Casilla 160-C, Concepción, Chile.

E-mail address: ggatica@ci2ma.udec.cl

³ Department of Mathematics, Simon Fraser University, 8888 University Drive, Burnaby, BC V5A 1S6, Canada.

E-mail address: smoragas@sfu.ca

⁴ School of Mathematics, Monash University, 9 Rainforest Walk, Clayton, VIC 3800, Australia.

E-mail address: ricardo.ruizbaier@monash.edu.

Abstract. A new fully-mixed formulation is advanced for the stationary Oberbeck–Boussinesq problem when viscosity depends on both temperature and concentration of a solute. Following recent ideas in the context of mixed methods for Boussinesq and Navier–Stokes systems, the velocity gradient and the Bernoulli stress tensor are taken as additional field variables in the momentum and mass equilibrium equations. Similarly, the gradients of temperature and concentration together with a Bernoulli vector are considered as unknowns in the heat and mass transfer equations. Consequently, a dual-mixed approach with Dirichlet data is defined in each sub-system, and the well-known Banach and Brouwer theorems are combined with Babuška–Brezzi’s theory in each independent set of equations, yielding the solvability of the continuous and discrete schemes. We show that our development also applies to the case where the equations of thermal energy and solute transport are coupled through cross-diffusion. Appropriate finite element subspaces are specified, and optimal a priori error estimates are derived. Furthermore, a reliable and efficient residual-based a posteriori error estimator is proposed. Several numerical examples illustrate the performance of the fully-mixed scheme and of the adaptive refinement algorithm driven by the error estimator.

2020 Mathematics Subject Classification. 65N30, 65N12, 65N15, 35Q79, 80A20, 76D05, 76R10.

Keywords. Oberbeck–Boussinesq equations, fully-mixed formulation, fixed-point theory, finite element methods, a priori error analysis.

1. Introduction

Natural convection in porous media is of paramount interest due to its applicability in many environmental and technological processes. Typical examples include seawater flow, mantle flow in the earth’s crust, water movement in geothermal reservoirs, underground spreading of chemical wastes and other pollutants, and many others [1, 3, 19, 38, 40]. A special case is when temperature and concentration differences occur simultaneously, and a mathematical description of this flow regime is the so-called

This research was partially supported by CONICYT-Chile through the project AFB170001 of the PIA Program: Concurso Apoyo a Centros Científicos y Tecnológicos de Excelencia con Financiamiento Basal and by the Fondecyt project 11190241; by Centro de Investigación en Ingeniería Matemática (CI²MA), Universidad de Concepción; by Proyecto de Fondos Especiales DIUBB 185709 3/FE of the Universidad del Bío-Bío; and by the HPC-Europa3 Transnational Access Grant HPC175QA9K.

Oberbeck–Boussinesq approximation. It consists of the incompressible Navier–Stokes/Brinkman equations describing the hydrodynamics of viscous flow in the porous media, and advection-diffusion equations for solute’s concentration and temperature, nonlinearly coupled via convective mass and heat transfer.

Motivated by the vast applications and the challenging mathematical structure of such nonlinearly coupled system, the interest in analyzing it and in developing efficient numerical techniques to simulate related phenomena has significantly increased, see, e.g., [2, 4, 5, 7, 9, 11, 14, 16, 21, 22, 25, 28, 29, 32, 34, 36, 39, 42, 41, 44, 46, 48] and the references therein. Those works include numerical algorithms based on finite volume approaches, standard finite element techniques, parallel and projection-based stabilization methods, spectral collocation, and mixed finite element methods; and they concentrate on heat-driven flows and double-diffusion convection, including cases in which the phenomena occur in porous enclosures, with either constant or variable physical parameters.

In certain applications, additional physically relevant variables, such as the velocity gradient or the concentration and heat fluxes, might reveal specific mechanisms of the phenomena, and hence become of primary interest. Whilst these variables could be obtained via numerical differentiation of the discrete solutions provided by standard methods, this entails a loss of accuracy that deteriorate the expected convergence orders. In light of this, the purpose of this work is to construct, analyze and implement a high-order optimally convergent mixed finite element scheme for simulating this type of coupled flows. We extend the use of the theory developed in the recent work [22] (specified for temperature-driven flows), to the case of Oberbeck–Boussinesq equations. In doing so, and besides the stress and the velocity gradient in the fluid equations, we introduce the temperature gradient, the concentration gradient and a vector version of the Bernoulli tensor combining advective and diffusive heat and concentration fluxes, as further field variables. The extension is non-trivial, but the resulting formulation retains the same saddle-point structure on reflexive Banach spaces for both the Navier–Stokes/Darcy and the thermal energy conservation equations. This feature constitutes a clear (but essentially theoretically relevant) advantage over recent developments since the continuous and discrete analyses for the two sub-models can be carried out separately and very much in the same way. Indeed, the well-known Banach and Brouwer theorems, combined with the application of the Babuška–Brezzi theory to each independent equation, lead to the solvability of the continuous and discrete schemes. Additionally, our analysis is also applicable to a case of cross-diffusion for the heat and mass transfer equations. In this regard, we emphasize that, rather than deriving a new theoretical framework, in the present work we show that the same theory of [22] can be extended accordingly and tailored to fit the Oberbeck–Boussinesq model, thus confirming its applicability to a larger family of nonlinear coupled problems. Appropriate finite element spaces (that yield a stable Galerkin scheme) are, for instance, Raviart–Thomas elements of order $k \geq n - 1$ for the Bernoulli tensor and its vector version, and piecewise polynomials (and not necessarily globally continuous) of degree $\leq k$ for the velocity, the temperature, the concentration, and all gradients, constitute a feasible choice yielding a stable Galerkin scheme. Discontinuous approximations can be of interest if rough solutions or coefficients are expected. Some advantages of the proposed scheme include

- (a) the pressure is eliminated by the functional setting, and it can be recovered by postprocessing,
- (b) relaxed regularity requirements on temperature and concentration, yielding more flexibility in choosing approximation spaces,
- (c) the trace-free velocity gradient and the temperature and concentration gradients are now primary unknowns,

- (d) differently from the methods constructed in [11, 16, 24, 41], the Dirichlet boundary conditions for the temperature and concentration are naturally introduced into the formulation, avoiding the use of either an extension or a boundary Lagrange multiplier,
- (e) this scheme does not involve any augmentation term (as done, e.g. in [6, 7, 9, 10]), avoiding stabilization parameters for well-posedness of the continuous and discrete problems, as well as for the convergence of the method,
- (f) the analysis also applies to a more general model of cross-diffusion.

The rest of this work is laid out as follows. At the end of this section we collect notational conventions. In Section 2 we state the governing equations in strong primal form and in strong mixed form. Next, the continuous variational formulation is derived in Section 3, which, after decoupling the fluid equation from the heat and mass transfer equations, is rewritten as a fixed-point operator equation. The solvability analysis is done using the Banach version of the classical Babuška–Brezzi theory, and the Banach fixed-point theorem. Also, we show that the same theory can be applied to a case of cross-diffusion. In Section 4 we define the Galerkin scheme with arbitrary finite element subspaces satisfying general assumptions, and follow basically the same techniques employed in Section 3 to analyze its solvability. We then specify finite element subspaces satisfying the assumptions stipulated in Section 4. Our analysis makes use of a sufficiency result developed in [22] (see, also [35]) for the occurrence of inf-sup conditions on products of reflexive Banach spaces. In Section 5 we assume sufficiently small data to derive an a priori error estimate for the Galerkin scheme with arbitrary finite element subspaces. A reliable and efficient residual-based a posteriori error estimator Ψ and its associated adaptive refinement algorithm are discussed in Section 6. Finally, numerical examples illustrating the performance of our fully-mixed formulation with the particular subspaces proposed in Section 4, and confirming the reliability and efficiency of Ψ , are reported in Section 7.

Recurrent notation and preliminaries

Let us denote by $\Omega \subseteq \mathbb{R}^n$, $n \in \{2, 3\}$ a given bounded domain with polyhedral boundary Γ , and denote by $\boldsymbol{\nu}$ the outward unit normal vector on Γ . Standard notation will be adopted for Lebesgue spaces $L^p(\Omega)$ and Sobolev spaces $W^{s,p}(\Omega)$, with $s \in \mathbb{R}$ and $p > 1$, whose corresponding norms, either for the scalar, vectorial, or tensorial case, are denoted by $\|\cdot\|_{0,p;\Omega}$ and $\|\cdot\|_{s,p;\Omega}$, respectively. In particular, given a non-negative integer m , $W^{m,2}(\Omega)$ is also denoted by $H^m(\Omega)$, and the notations of its norm and seminorm are simplified to $\|\cdot\|_{m,\Omega}$ and $|\cdot|_{m,\Omega}$, respectively. Furthermore, as usual \mathbb{I} stands for the identity tensor in $\mathbb{R}^{n \times n}$, and $|\cdot|$ denotes the Euclidean norm in \mathbb{R}^n . In turn, for any vector fields $\mathbf{v} = (v_i)_{i=1,n}$ and $\mathbf{w} = (w_i)_{i=1,n}$ we set the tensor product operator as $\mathbf{v} \otimes \mathbf{w} := (v_i w_j)_{i,j=1,n}$. In addition, for any tensor fields $\boldsymbol{\tau} = (\tau_{ij})_{i,j=1,n}$ and $\boldsymbol{\zeta} = (\zeta_{ij})_{i,j=1,n}$, we let $\mathbf{div}(\boldsymbol{\tau})$ be the divergence operator \mathbf{div} acting along the rows of $\boldsymbol{\tau}$, and denote by $\boldsymbol{\tau}^t$, $\text{tr}(\boldsymbol{\tau})$, and $\boldsymbol{\tau}^d$, the transpose, the trace, and the deviatoric tensor of $\boldsymbol{\tau}$, respectively, and define the tensor inner product between $\boldsymbol{\tau}$ and $\boldsymbol{\zeta}$ as $\boldsymbol{\tau} : \boldsymbol{\zeta} := \sum_{i,j=1}^n \tau_{ij} \zeta_{ij}$. Next, we introduce the Banach spaces $\mathbf{H}(\mathbf{div}_{4/3}; \Omega) := \left\{ \boldsymbol{\tau} \in \mathbf{L}^2(\Omega) : \mathbf{div}(\boldsymbol{\tau}) \in \mathbf{L}^{4/3}(\Omega) \right\}$ and $\mathbb{H}(\mathbf{div}_{4/3}; \Omega) := \left\{ \boldsymbol{\tau} \in \mathbb{L}^2(\Omega) : \mathbf{div}(\boldsymbol{\tau}) \in \mathbf{L}^{4/3}(\Omega) \right\}$, equipped with the natural norms

$$\|\boldsymbol{\tau}\|_{\mathbf{div}_{4/3};\Omega} := \|\boldsymbol{\tau}\|_{0,\Omega} + \|\mathbf{div}(\boldsymbol{\tau})\|_{0,4/3;\Omega} \quad \text{and} \quad \|\boldsymbol{\tau}\|_{\mathbb{div}_{4/3};\Omega} := \|\boldsymbol{\tau}\|_{0,\Omega} + \|\mathbf{div}(\boldsymbol{\tau})\|_{0,4/3;\Omega}.$$

In addition, $H^{1/2}(\Gamma)$ is the space of traces of functions of $H^1(\Omega)$ and $H^{-1/2}(\Gamma)$ is its dual. Also, by $\langle \cdot, \cdot \rangle_{\Gamma}$ we will denote the duality pairing between $\mathbf{H}^{-1/2}(\Gamma)$ and $\mathbf{H}^{1/2}(\Gamma)$ (and also between $H^{-1/2}(\Gamma)$ and $H^{1/2}(\Gamma)$).

2. Governing equations

The stationary Oberbeck–Boussinesq problem is constituted by the incompressible Navier–Stokes–Brinkman equations coupled with the heat and mass transfer equations through a convective term and a buoyancy term acting in opposite direction to gravity. The problem of interest (without dimensionless numbers for readability purposes) reduces to: Find a velocity field \mathbf{u} , a pressure field p , a temperature field φ_1 and a concentration field φ_2 , both defining a vector $\boldsymbol{\varphi} := (\varphi_1, \varphi_2)$, such that

$$\begin{aligned} \gamma \mathbf{u} - 2 \operatorname{div}(\mu(\boldsymbol{\varphi})\mathbf{e}(\mathbf{u})) + (\nabla \mathbf{u})\mathbf{u} + \nabla p - (\boldsymbol{\vartheta} \cdot \boldsymbol{\varphi})\mathbf{g} &= \mathbf{0} & \text{in } \Omega, \\ \operatorname{div} \mathbf{u} &= 0 & \text{in } \Omega, \\ -\operatorname{div}(\mathbb{K}_1 \nabla \varphi_1) + \mathbf{u} \cdot \nabla \varphi_1 &= 0 & \text{in } \Omega, \\ -\operatorname{div}(\mathbb{K}_2 \nabla \varphi_2) + \mathbf{u} \cdot \nabla \varphi_2 &= 0 & \text{in } \Omega, \end{aligned} \tag{2.1}$$

where γ is a positive constant inversely proportional to the reciprocal of the Darcy number Da , $\mu : \mathbb{R} \times \mathbb{R}^+ \rightarrow \mathbb{R}^+$ is the viscosity of the fluid, which is assumed to depend on both the temperature and the concentration of mass, $\mathbf{e}(\mathbf{u}) := \frac{1}{2}\{\nabla \mathbf{u} + (\nabla \mathbf{u})^\mathbf{t}\}$ is the rate of strain tensor, $\boldsymbol{\vartheta} := (\vartheta_1, \vartheta_2)$ is a vector containing expansion coefficients, $\mathbf{g} \in \mathbf{L}^\infty(\Omega)$ is an external force per unit mass, and $\mathbb{K}_j \in \mathbb{L}^\infty(\Omega)$, $j \in \{1, 2\}$, are uniformly positive definite tensors allowing the possibility of anisotropy (cf. [37]). In addition, μ is assumed bounded and Lipschitz continuous, i.e., there exist $\mu_1, \mu_2, L_\mu > 0$, such that

$$\mu_1 \leq \mu(\boldsymbol{\phi}) \leq \mu_2 \quad \text{and} \quad |\mu(\boldsymbol{\phi}) - \mu(\boldsymbol{\psi})| \leq L_\mu |\boldsymbol{\phi} - \boldsymbol{\psi}| \quad \forall \boldsymbol{\phi}, \boldsymbol{\psi} \in \mathbb{R} \times \mathbb{R}^+, \tag{2.2}$$

where $|\cdot|$ denotes from on the euclidean norm of \mathbb{R}^n , $n \in \{1, 2, 3\}$. Equations (2.1) are complemented with Dirichlet boundary conditions for the velocity, the temperature, and the concentration, that is

$$\mathbf{u} = \mathbf{u}_D, \quad \varphi_1 = \varphi_{1,D}, \quad \text{and} \quad \varphi_2 = \varphi_{2,D} \quad \text{on } \Gamma, \tag{2.3}$$

with given data $\mathbf{u}_D \in \mathbf{H}^{1/2}(\Gamma)$, $\varphi_{1,D} \in H^{1/2}(\Gamma)$ and $\varphi_{2,D} \in H^{1/2}(\Gamma)$. Owing to the incompressibility of the fluid and the Dirichlet boundary condition for \mathbf{u} , the datum \mathbf{u}_D must satisfy the compatibility condition $\int_\Gamma \mathbf{u}_D \cdot \boldsymbol{\nu} = 0$. In addition, due to the first equation of (2.1), and in order to guarantee uniqueness of the pressure, this unknown will be sought in the space

$$L_0^2(\Omega) := \left\{ q \in L^2(\Omega) : \int_\Omega q = 0 \right\}.$$

On the other hand, in order to derive a fully-mixed formulation for (2.1)–(2.3), in which the essential boundary conditions become natural ones, we now proceed as in [22, Section 2] (see also [7, 23, 24]), and introduce the velocity gradient and the Bernoulli stress tensor as further unknowns

$$\mathbf{t} := \nabla \mathbf{u} \quad \text{and} \quad \boldsymbol{\sigma} := 2\mu(\boldsymbol{\varphi})\mathbf{t}_{sym} - \frac{1}{2}(\mathbf{u} \otimes \mathbf{u}) - p\mathbf{I}, \tag{2.4}$$

where $\mathbf{t}_{sym} := \frac{1}{2}\{\mathbf{t} + \mathbf{t}^\mathbf{t}\}$ is the symmetric part of \mathbf{t} . In this way, and noting thanks to the incompressibility condition that $\operatorname{div}(\mathbf{u} \otimes \mathbf{u}) = (\nabla \mathbf{u})\mathbf{u}$, we find that the first equation of (2.1) becomes

$$\gamma \mathbf{u} - \operatorname{div} \boldsymbol{\sigma} + \frac{1}{2}\mathbf{t}\mathbf{u} - (\boldsymbol{\vartheta} \cdot \boldsymbol{\varphi})\mathbf{g} = \mathbf{0}.$$

In turn, applying the matrix trace to the expression defining $\boldsymbol{\sigma}$ and using that $\operatorname{tr}(\mathbf{t}_{sym}) = \operatorname{div} \mathbf{u} = 0$, one arrives at

$$p = -\frac{1}{2n}\operatorname{tr}(2\boldsymbol{\sigma} + \mathbf{u} \otimes \mathbf{u}), \tag{2.5}$$

which, replaced back into the second equation of (2.4), yields what we call from now on the new constitutive law of the fluid, namely

$$\boldsymbol{\sigma}^d = 2\mu(\boldsymbol{\varphi})\mathbf{t}_{sym} - \frac{1}{2}(\mathbf{u} \otimes \mathbf{u})^d. \quad (2.6)$$

Conversely, starting from (2.5) and (2.6) we readily recover the incompressibility condition and the original definition of $\boldsymbol{\sigma}$, whence these pair of equations are actually equivalent. Furthermore, for the heat and mass transfer equations we proceed similarly as for the fluid, so that following now [22, eq. (2.7)], we introduce for each $j \in \{1, 2\}$ the auxiliary unknowns

$$\tilde{\mathbf{t}}_j := \nabla \varphi_j \quad \text{and} \quad \tilde{\boldsymbol{\sigma}}_j := \mathbb{K}_j \tilde{\mathbf{t}}_j - \frac{1}{2} \varphi_j \mathbf{u}. \quad (2.7)$$

They represent respectively the gradients and the total (diffusive plus advective) fluxes for temperature and concentration of solutes. Observing again from the incompressibility condition that in this case there holds $\mathbf{div}(\varphi_j \mathbf{u}) = \nabla \varphi_j \cdot \mathbf{u} = \tilde{\mathbf{t}}_j \cdot \mathbf{u}$, our model problem (2.1) is re-stated as follows: Find $(\mathbf{u}, \mathbf{t}, \boldsymbol{\sigma})$ and $(\varphi_j, \tilde{\mathbf{t}}_j, \tilde{\boldsymbol{\sigma}}_j)$, $j \in \{1, 2\}$, in suitable spaces to be indicated below such that

$$\begin{aligned} \nabla \mathbf{u} &= \mathbf{t} && \text{in } \Omega, \\ \gamma \mathbf{u} - \mathbf{div} \boldsymbol{\sigma} + \frac{1}{2} \mathbf{t} \mathbf{u} - (\boldsymbol{\vartheta} \cdot \boldsymbol{\varphi}) \mathbf{g} &= \mathbf{0} && \text{in } \Omega, \\ 2\mu(\boldsymbol{\varphi})\mathbf{t}_{sym} - \frac{1}{2}(\mathbf{u} \otimes \mathbf{u})^d &= \boldsymbol{\sigma}^d && \text{in } \Omega, \\ \nabla \varphi_j &= \tilde{\mathbf{t}}_j && \text{in } \Omega, \\ \mathbb{K}_j \tilde{\mathbf{t}}_j - \frac{1}{2} \varphi_j \mathbf{u} &= \tilde{\boldsymbol{\sigma}}_j && \text{in } \Omega, \\ -\mathbf{div} \tilde{\boldsymbol{\sigma}}_j + \frac{1}{2} \tilde{\mathbf{t}}_j \cdot \mathbf{u} &= 0 && \text{in } \Omega, \\ \mathbf{u} = \mathbf{u}_D \quad \text{and} \quad \boldsymbol{\varphi} = \boldsymbol{\varphi}_D &&& \text{on } \Gamma, \\ \int_{\Omega} \text{tr}(2\boldsymbol{\sigma} + \mathbf{u} \otimes \mathbf{u}) &= 0, \end{aligned} \quad (2.8)$$

where the Dirichlet datum for $\boldsymbol{\varphi}$ is certainly given by $\boldsymbol{\varphi}_D := (\varphi_{1,D}, \varphi_{2,D})$. As suggested by (2.5), p is eliminated from the formulation and computed afterwards in terms of $\boldsymbol{\sigma}$ and \mathbf{u} . This fact justifies the last equation in (2.8), which aims to ensure that the resulting p does belong to $L_0^2(\Omega)$.

3. Well-posedness of the continuous problem

In this section we derive a weak formulation for (2.8) and analyze its properties decoupling the advection-diffusion equations from the fluid equations using a fixed-point argument. The main differences with respect to [22, eq. (2.8)] reside in the presence of an extra first order term $\gamma \mathbf{u}$ and the mass transfer equation, but the overall structure of the problem remains unchanged.

3.1. The fully-mixed formulation

Proceeding in a standard manner, we arrive at the following weak form of (2.8): Find $(\mathbf{u}, \mathbf{t}, \boldsymbol{\sigma}) \in \mathbf{L}^4(\Omega) \times \mathbf{L}_{\text{tr}}^2(\Omega) \times \mathbb{H}(\mathbf{div}_{4/3}; \Omega)$, and $(\varphi_j, \tilde{\mathbf{t}}_j, \tilde{\boldsymbol{\sigma}}_j) \in L^4(\Omega) \times \mathbf{L}^2(\Omega) \times \mathbf{H}(\text{div}_{4/3}; \Omega)$, $j \in \{1, 2\}$, such that

$\int_{\Omega} \operatorname{tr}(2\boldsymbol{\sigma} + \mathbf{u} \otimes \mathbf{u}) = 0$, and

$$\begin{aligned}
 \int_{\Omega} \gamma \mathbf{u} \cdot \mathbf{v} - \int_{\Omega} \mathbf{v} \cdot \operatorname{div}(\boldsymbol{\sigma}) + \frac{1}{2} \int_{\Omega} \mathbf{t} \mathbf{u} \cdot \mathbf{v} &= \int_{\Omega} (\boldsymbol{\vartheta} \cdot \boldsymbol{\varphi}) \mathbf{g} \cdot \mathbf{v} & \forall \mathbf{v} \in \mathbf{L}^4(\Omega), \\
 \int_{\Omega} 2\mu(\boldsymbol{\varphi}) \mathbf{t}_{sym} : \mathbf{s} - \frac{1}{2} \int_{\Omega} (\mathbf{u} \otimes \mathbf{u})^d : \mathbf{s}^d &= \int_{\Omega} \boldsymbol{\sigma}^d : \mathbf{s}^d & \forall \mathbf{s} \in \mathbb{L}_{\operatorname{tr}}^2(\Omega), \\
 \int_{\Omega} \boldsymbol{\tau} : \mathbf{t} + \int_{\Omega} \mathbf{u} \cdot \operatorname{div}(\boldsymbol{\tau}) &= \langle \boldsymbol{\tau} \boldsymbol{\nu}, \mathbf{u}_D \rangle_{\Gamma} & \forall \boldsymbol{\tau} \in \mathbb{H}(\operatorname{div}_{4/3}; \Omega), \\
 - \int_{\Omega} \psi_j \operatorname{div}(\tilde{\boldsymbol{\sigma}}_j) + \frac{1}{2} \int_{\Omega} \psi_j \tilde{\mathbf{t}}_j \cdot \mathbf{u} &= 0 & \forall \psi_j \in L^4(\Omega), \\
 \int_{\Omega} \mathbb{K}_j \tilde{\mathbf{t}}_j \cdot \tilde{\mathbf{s}}_j - \frac{1}{2} \int_{\Omega} \varphi_j \mathbf{u} \cdot \tilde{\mathbf{s}}_j &= \int_{\Omega} \tilde{\boldsymbol{\sigma}}_j \cdot \tilde{\mathbf{s}}_j & \forall \tilde{\mathbf{s}}_j \in \mathbf{L}^2(\Omega), \\
 \int_{\Omega} \tilde{\boldsymbol{\tau}}_j \cdot \tilde{\mathbf{t}}_j + \int_{\Omega} \varphi_j \operatorname{div}(\tilde{\boldsymbol{\tau}}_j) &= \langle \tilde{\boldsymbol{\tau}}_j \cdot \boldsymbol{\nu}, \varphi_j, D \rangle_{\Gamma} & \forall \tilde{\boldsymbol{\tau}}_j \in \mathbf{H}(\operatorname{div}_{4/3}; \Omega),
 \end{aligned} \tag{3.1}$$

where the Dirichlet boundary conditions for \mathbf{u} and $\boldsymbol{\varphi}$ have been employed in the derivation of the foregoing weak formulation. Note here that the continuous injection of $\mathbf{H}^1(\Omega)$ in $\mathbf{L}^4(\Omega)$ (resp. the continuous injection of $\mathbf{H}^1(\Omega)$ in $L^4(\Omega)$) guarantees that $\boldsymbol{\tau} \boldsymbol{\nu}$ (resp. $\tilde{\boldsymbol{\tau}}_j \cdot \boldsymbol{\nu}$) is well defined and belongs to $\mathbf{H}^{-1/2}(\Gamma)$ (resp. $\mathbf{H}^{-1/2}(\Gamma)$) when $\boldsymbol{\tau} \in \mathbb{H}(\operatorname{div}_{4/3}; \Omega)$ (resp. $\tilde{\boldsymbol{\tau}}_j \in \mathbf{H}(\operatorname{div}_{4/3}; \Omega)$). On the other hand, notice that we look for \mathbf{t} in $\mathbb{L}_{\operatorname{tr}}^2(\Omega)$ due to the incompressibility condition, where

$$\mathbb{L}_{\operatorname{tr}}^2(\Omega) := \left\{ \mathbf{s} \in \mathbb{L}^2 : \operatorname{tr}(\mathbf{s}) = 0 \right\}.$$

We now consider, as in [22, eqs. (3.8) and (3.9)], the orthogonal decomposition (cf., e.g. [30, 43])

$$\mathbb{H}(\operatorname{div}_{4/3}; \Omega) = \mathbb{H}_0(\operatorname{div}_{4/3}; \Omega) \oplus \mathbb{R}\mathbb{I}, \quad \text{with } \mathbb{H}_0(\operatorname{div}_{4/3}; \Omega) := \left\{ \boldsymbol{\zeta} \in \mathbb{H}(\operatorname{div}_{4/3}; \Omega) : \int_{\Omega} \operatorname{tr}(\boldsymbol{\zeta}) = 0 \right\}, \tag{3.2}$$

and (3.2) together with $\int_{\Omega} \operatorname{tr}(2\boldsymbol{\sigma} + \mathbf{u} \otimes \mathbf{u}) = 0$, imply that $\boldsymbol{\sigma}$ can be uniquely decomposed as

$$\boldsymbol{\sigma} = \boldsymbol{\sigma}_0 + c_0 \mathbb{I}, \quad \text{with } \boldsymbol{\sigma}_0 \in \mathbb{H}_0(\operatorname{div}_{4/3}; \Omega) \quad \text{and} \quad c_0 := -\frac{1}{2n|\Omega|} \int_{\Omega} \operatorname{tr}(\mathbf{u} \otimes \mathbf{u}). \tag{3.3}$$

Making abuse of notation, we will continue to denote $\boldsymbol{\sigma}_0$ as simply $\boldsymbol{\sigma} \in \mathbb{H}_0(\operatorname{div}_{4/3}; \Omega)$, and instead of (3.1) consider the equivalent formulation: Find $(\mathbf{u}, \mathbf{t}, \boldsymbol{\sigma}) \in \mathbf{L}^4(\Omega) \times \mathbb{L}_{\operatorname{tr}}^2(\Omega) \times \mathbb{H}_0(\operatorname{div}_{4/3}; \Omega)$, and $(\varphi_j, \tilde{\mathbf{t}}_j, \tilde{\boldsymbol{\sigma}}_j) \in L^4(\Omega) \times \mathbf{L}^2(\Omega) \times \mathbf{H}(\operatorname{div}_{4/3}; \Omega)$, $j \in \{1, 2\}$, such that (3.1) holds for all $(\mathbf{v}, \mathbf{s}, \boldsymbol{\tau}) \in \mathbf{L}^4(\Omega) \times \mathbb{L}_{\operatorname{tr}}^2(\Omega) \times \mathbb{H}_0(\operatorname{div}_{4/3}; \Omega)$, and $(\psi_j, \tilde{\mathbf{s}}_j, \tilde{\boldsymbol{\tau}}_j) \in L^4(\Omega) \times \mathbf{L}^2(\Omega) \times \mathbf{H}(\operatorname{div}_{4/3}; \Omega)$, $j \in \{1, 2\}$. For sake of clarity in the presentation we introduce the following vector quantities

$$\vec{\mathbf{u}} := (\mathbf{u}, \mathbf{t}), \quad \vec{\mathbf{v}} := (\mathbf{v}, \mathbf{s}), \quad \vec{\mathbf{u}}_0 := (\mathbf{u}_0, \mathbf{t}_0) \in \mathbf{L}^4(\Omega) \times \mathbb{L}_{\operatorname{tr}}^2(\Omega),$$

and

$$\vec{\boldsymbol{\varphi}}_j := (\varphi_j, \tilde{\mathbf{t}}_j), \quad \vec{\boldsymbol{\psi}}_j := (\psi_j, \tilde{\mathbf{s}}_j) \in L^4(\Omega) \times \mathbf{L}^2(\Omega),$$

with their corresponding norms given by

$$\|\vec{\mathbf{u}}\| := \|\mathbf{u}\|_{0,4;\Omega} + \|\mathbf{t}\|_{0,\Omega} \quad \forall \vec{\mathbf{u}} \in \mathbf{L}^4(\Omega) \times \mathbb{L}_{\operatorname{tr}}^2(\Omega), \tag{3.4}$$

$$\|\vec{\boldsymbol{\varphi}}_j\| := \|\varphi_j\|_{0,4;\Omega} + \|\tilde{\mathbf{t}}_j\|_{0,\Omega} \quad \forall \vec{\boldsymbol{\varphi}}_j \in L^4(\Omega) \times \mathbf{L}^2(\Omega). \tag{3.5}$$

Then, the fully-mixed formulation for the coupled problem reads: Find $(\vec{\mathbf{u}}, \boldsymbol{\sigma}) \in (\mathbf{L}^4(\Omega) \times \mathbb{L}_{\text{tr}}^2(\Omega)) \times \mathbb{H}_0(\mathbf{div}_{4/3}; \Omega)$ and $(\vec{\boldsymbol{\varphi}}_j, \vec{\boldsymbol{\sigma}}_j) \in (\mathbf{L}^4(\Omega) \times \mathbf{L}^2(\Omega)) \times \mathbf{H}(\mathbf{div}_{4/3}; \Omega)$, $j \in \{1, 2\}$, such that

$$\begin{aligned} a_\varphi(\vec{\mathbf{u}}, \vec{\mathbf{v}}) + c(\mathbf{u}; \vec{\mathbf{u}}, \vec{\mathbf{v}}) + b(\vec{\mathbf{v}}, \boldsymbol{\sigma}) &= F_\varphi(\vec{\mathbf{v}}) \quad \forall \vec{\mathbf{v}} \in (\mathbf{L}^4(\Omega) \times \mathbb{L}_{\text{tr}}^2(\Omega)), \\ b(\vec{\mathbf{u}}, \boldsymbol{\tau}) &= G(\boldsymbol{\tau}) \quad \forall \boldsymbol{\tau} \in \mathbb{H}_0(\mathbf{div}_{4/3}; \Omega), \\ \tilde{a}_j(\vec{\boldsymbol{\varphi}}_j, \vec{\boldsymbol{\psi}}_j) + \tilde{c}_\mathbf{u}(\vec{\boldsymbol{\varphi}}_j, \vec{\boldsymbol{\psi}}_j) + \tilde{b}(\vec{\boldsymbol{\psi}}_j, \vec{\boldsymbol{\sigma}}_j) &= 0 \quad \forall \vec{\boldsymbol{\psi}}_j \in (\mathbf{L}^4(\Omega) \times \mathbf{L}^2(\Omega)), \\ \tilde{b}(\vec{\boldsymbol{\varphi}}_j, \vec{\boldsymbol{\tau}}_j) &= \tilde{G}_j(\vec{\boldsymbol{\tau}}_j) \quad \forall \vec{\boldsymbol{\tau}}_j \in \mathbf{H}(\mathbf{div}_{4/3}; \Omega), \end{aligned} \quad (3.6)$$

where, given arbitrary $(\mathbf{w}, \phi) \in \mathbf{L}^4(\Omega) \times \mathbf{L}^4(\Omega)$, the forms a_ϕ , b , $c(\mathbf{w}; \cdot, \cdot)$, \tilde{a}_j , \tilde{b} , and $\tilde{c}_\mathbf{w}$, and the functionals F_ϕ , G , and \tilde{G}_j , are defined by

$$a_\phi(\vec{\mathbf{u}}, \vec{\mathbf{v}}) := \int_\Omega \gamma \mathbf{u} \cdot \mathbf{v} + \int_\Omega 2\mu(\phi) \mathbf{t}_{\text{sym}} : \mathbf{s}, \quad b(\vec{\mathbf{v}}, \boldsymbol{\tau}) := - \int_\Omega \boldsymbol{\tau} : \mathbf{s} - \int_\Omega \mathbf{v} \cdot \mathbf{div}(\boldsymbol{\tau}), \quad (3.7)$$

$$c(\mathbf{w}; \vec{\mathbf{u}}, \vec{\mathbf{v}}) := \frac{1}{2} \left\{ \int_\Omega \mathbf{t} \mathbf{w} \cdot \mathbf{v} - \int_\Omega (\mathbf{u} \otimes \mathbf{w})^{\text{d}} : \mathbf{s}^{\text{d}} \right\}, \quad (3.8)$$

for all $\vec{\mathbf{u}} := (\mathbf{u}, \mathbf{t})$, $\vec{\mathbf{v}} := (\mathbf{v}, \mathbf{s}) \in \mathbf{L}^4(\Omega) \times \mathbb{L}_{\text{tr}}^2(\Omega)$, for all $\boldsymbol{\tau} \in \mathbb{H}_0(\mathbf{div}_{4/3}; \Omega)$,

$$\begin{aligned} \tilde{a}_j(\vec{\boldsymbol{\varphi}}_j, \vec{\boldsymbol{\psi}}_j) &:= \int_\Omega \mathbb{K}_j \tilde{\mathbf{t}}_j \cdot \tilde{\mathbf{s}}_j, \quad \tilde{b}(\vec{\boldsymbol{\psi}}_j, \vec{\boldsymbol{\tau}}_j) := - \int_\Omega \tilde{\boldsymbol{\tau}}_j \cdot \tilde{\mathbf{s}}_j - \int_\Omega \psi_j \mathbf{div}(\tilde{\boldsymbol{\tau}}_j), \\ \tilde{c}_\mathbf{w}(\vec{\boldsymbol{\varphi}}_j, \vec{\boldsymbol{\psi}}_j) &:= \frac{1}{2} \left\{ \int_\Omega \psi_j \tilde{\mathbf{t}}_j \cdot \mathbf{w} - \int_\Omega \varphi_j \mathbf{w} \cdot \tilde{\mathbf{s}}_j \right\}, \end{aligned} \quad (3.9)$$

for all $\vec{\boldsymbol{\varphi}}_j := (\varphi_j, \tilde{\mathbf{t}}_j)$, $\vec{\boldsymbol{\psi}}_j := (\psi_j, \tilde{\mathbf{s}}_j) \in \mathbf{L}^4(\Omega) \times \mathbf{L}^2(\Omega)$, for all $\tilde{\boldsymbol{\tau}}_j \in \mathbf{H}(\mathbf{div}_{4/3}; \Omega)$, and

$$F_\phi(\vec{\mathbf{v}}) := \int_\Omega (\boldsymbol{\vartheta} \cdot \phi) \mathbf{g} \cdot \mathbf{v}, \quad G(\boldsymbol{\tau}) := - \langle \boldsymbol{\tau} \nu, \mathbf{u}_D \rangle_\Gamma, \quad \tilde{G}_j(\vec{\boldsymbol{\tau}}_j) := - \langle \tilde{\boldsymbol{\tau}}_j \cdot \nu, \varphi_{j,D} \rangle_\Gamma, \quad (3.10)$$

for all $\vec{\mathbf{v}} := (\mathbf{v}, \mathbf{s}) \in \mathbf{L}^4(\Omega) \times \mathbb{L}_{\text{tr}}^2(\Omega)$, for all $\boldsymbol{\tau} \in \mathbb{H}_0(\mathbf{div}_{4/3}; \Omega)$, for all $\tilde{\boldsymbol{\tau}}_j \in \mathbf{H}(\mathbf{div}_{4/3}; \Omega)$.

In what follows we proceed similarly as in [10] to prove that problem (3.6) is well-posed. More precisely, in Section 3.2 we will reformulate (3.6) as an equivalent fixed-point equation in terms of a suitable operator T . Then, in Section 3.3 we show that T is well-defined, and finally in Section 3.4 we apply the classical Banach theorem to conclude that T has a unique fixed point.

3.2. The fixed-point approach

We first let $S : \mathbf{L}^4(\Omega) \times \mathbf{L}^4(\Omega) \longrightarrow \mathbf{L}^4(\Omega)$ be the operator defined by

$$S(\mathbf{w}, \phi) := \mathbf{u} \quad \forall (\mathbf{w}, \phi) \in \mathbf{L}^4(\Omega) \times \mathbf{L}^4(\Omega),$$

where $(\vec{\mathbf{u}}, \boldsymbol{\sigma}) := ((\mathbf{u}, \mathbf{t}), \boldsymbol{\sigma}) \in (\mathbf{L}^4(\Omega) \times \mathbb{L}_{\text{tr}}^2(\Omega)) \times \mathbb{H}_0(\mathbf{div}_{4/3}; \Omega)$ is the unique solution (to be confirmed below) of the problem:

$$\begin{aligned} a_\phi(\vec{\mathbf{u}}, \vec{\mathbf{v}}) + c(\mathbf{w}; \vec{\mathbf{u}}, \vec{\mathbf{v}}) + b(\vec{\mathbf{v}}, \boldsymbol{\sigma}) &= F_\phi(\vec{\mathbf{v}}) \quad \forall \vec{\mathbf{v}} \in \mathbf{L}^4(\Omega) \times \mathbb{L}_{\text{tr}}^2(\Omega), \\ b(\vec{\mathbf{u}}, \boldsymbol{\tau}) &= G(\boldsymbol{\tau}) \quad \forall \boldsymbol{\tau} \in \mathbb{H}_0(\mathbf{div}_{4/3}; \Omega). \end{aligned} \quad (3.11)$$

In turn, for each $j \in \{1, 2\}$ we let $\tilde{S}_j : \mathbf{L}^4(\Omega) \longrightarrow \mathbf{L}^4(\Omega)$ be the operator given by

$$\tilde{S}_j(\mathbf{w}) := \varphi_j \quad \forall \mathbf{w} \in \mathbf{L}^4(\Omega),$$

where $(\vec{\varphi}_j, \vec{\sigma}_j) := ((\varphi_j, \tilde{\mathbf{t}}_j), \tilde{\sigma}_j) \in (\mathbf{L}^4(\Omega) \times \mathbf{L}^2(\Omega)) \times \mathbf{H}(\operatorname{div}_{4/3}; \Omega)$ is the unique solution (to be confirmed below) of the problem:

$$\begin{aligned} \tilde{a}_j(\vec{\varphi}_j, \vec{\psi}_j) + \tilde{c}_{\mathbf{w}}(\vec{\varphi}_j, \vec{\psi}_j) + \tilde{b}(\vec{\psi}_j, \vec{\sigma}_j) &= 0 & \forall \vec{\psi}_j \in \mathbf{L}^4(\Omega) \times \mathbf{L}^2(\Omega), \\ \tilde{b}(\vec{\varphi}_j, \vec{\tau}_j) &= \tilde{G}_j(\vec{\tau}_j) & \forall \vec{\tau}_j \in \mathbf{H}(\operatorname{div}_{4/3}; \Omega), \end{aligned} \quad (3.12)$$

so that we can introduce $\tilde{S}(\mathbf{w}) := (\tilde{S}_1(\mathbf{w}), \tilde{S}_2(\mathbf{w})) \in \mathbf{L}^4(\Omega)$ for all $\mathbf{w} \in \mathbf{L}^4(\Omega)$. Having defined the mappings S and \tilde{S} , we now set $T : \mathbf{L}^4(\Omega) \times \mathbf{L}^4(\Omega) \rightarrow \mathbf{L}^4(\Omega) \times \mathbf{L}^4(\Omega)$ as

$$T(\mathbf{w}, \phi) := (S(\mathbf{w}, \phi), \tilde{S}(S(\mathbf{w}, \phi))) \quad \forall (\mathbf{w}, \phi) \in \mathbf{L}^4(\Omega) \times \mathbf{L}^4(\Omega), \quad (3.13)$$

and realize that solving (3.6) is equivalent to finding $(\mathbf{u}, \varphi) \in \mathbf{L}^4(\Omega) \times \mathbf{L}^4(\Omega)$ such that

$$T(\mathbf{u}, \varphi) = (\mathbf{u}, \varphi).$$

3.3. Well-definedness of the fixed-point operator

In what follows we show that T is well-defined, reducing to prove that the uncoupled problems (3.11) and (3.12) are well-posed. These results will be straightforward consequences of the Banach version of the Babuška–Brezzi theory (cf. [27, Theorem 2.34]). Note that the problems in (3.12) only differ in the bilinear forms \tilde{a}_j and the functionals \tilde{G}_j on the right-hand side of the second equation. However, since the tensors \mathbb{K}_j defining the forms \tilde{a}_j satisfy exactly the same properties, the required hypotheses need to be checked only for a generic \tilde{a}_j and for \tilde{b} .

We begin our analysis by observing, as in [22, eqs. (3.30), (3.31)], that the kernels of the operators induced by the bilinear forms b and \tilde{b} , are given by \mathbf{V} and $\tilde{\mathbf{V}}$, respectively, where

$$\mathbf{V} := \left\{ \vec{\mathbf{v}} = (\mathbf{v}, \mathbf{s}) \in \mathbf{L}^4(\Omega) \times \mathbb{L}_{\operatorname{tr}}^2(\Omega) : \nabla \mathbf{v} = \mathbf{s} \quad \text{and} \quad \mathbf{v} \in \mathbf{H}_0^1(\Omega) \right\}, \quad (3.14)$$

and

$$\tilde{\mathbf{V}} := \left\{ \vec{\psi} = (\psi, \tilde{\mathbf{s}}) \in \mathbf{L}^4(\Omega) \times \mathbf{L}^2(\Omega) : \nabla \psi = \tilde{\mathbf{s}} \quad \text{and} \quad \psi \in \mathbf{H}_0^1(\Omega) \right\}. \quad (3.15)$$

Next, we introduce the spaces $\mathbf{H} := \mathbf{L}^4(\Omega) \times \mathbb{L}_{\operatorname{tr}}^2(\Omega)$ and $\tilde{\mathbf{H}} := \mathbf{L}^4(\Omega) \times \mathbf{L}^2(\Omega)$, with norms given by (3.4) and (3.5), and readily establish the boundedness of a_ϕ , b , \tilde{a}_j , and \tilde{b} , by using the Cauchy–Schwarz inequality, the bound for μ (cf. (2.2)), and the fact that $\mathbb{K}_j \in \mathbb{L}^\infty(\Omega)$. More precisely, there hold

$$a_\phi(\vec{\mathbf{u}}, \vec{\mathbf{v}}) \leq (|\Omega|^{1/2} \gamma + 2\mu_2) \|\vec{\mathbf{u}}\| \|\vec{\mathbf{v}}\| \quad \forall \phi \in \mathbf{L}^4(\Omega), \quad \forall \vec{\mathbf{u}}, \vec{\mathbf{v}} \in \mathbf{H}, \quad (3.16)$$

$$b(\vec{\mathbf{v}}, \boldsymbol{\tau}) \leq \|\vec{\mathbf{v}}\| \|\boldsymbol{\tau}\|_{\operatorname{div}_{4/3}; \Omega} \quad \forall \vec{\mathbf{v}} \in \mathbf{H}, \quad \forall \boldsymbol{\tau} \in \mathbb{H}_0(\operatorname{div}_{4/3}; \Omega), \quad (3.17)$$

$$\tilde{a}_j(\vec{\varphi}_j, \vec{\psi}_j) \leq \|\mathbb{K}_j\|_{0, \infty; \Omega} \|\vec{\varphi}_j\| \|\vec{\psi}_j\| \quad \forall \vec{\varphi}_j, \vec{\psi}_j \in \tilde{\mathbf{H}}, \quad (3.18)$$

$$\tilde{b}(\vec{\psi}_j, \vec{\tau}_j) \leq \|\vec{\psi}_j\| \|\vec{\tau}_j\|_{\operatorname{div}_{4/3}; \Omega} \quad \forall \vec{\psi}_j \in \tilde{\mathbf{H}}, \quad \forall \vec{\tau}_j \in \mathbf{H}(\operatorname{div}_{4/3}; \Omega). \quad (3.19)$$

In turn, the following lemma establishes the ellipticity of the bilinear forms a_ϕ and \tilde{a}_j .

Lemma 3.1. *There exist positive constants α and $\tilde{\alpha}$ such that*

$$a_\phi(\vec{\mathbf{v}}, \vec{\mathbf{v}}) \geq \alpha \|\vec{\mathbf{v}}\|^2 \quad \forall \phi \in \mathbf{L}^4(\Omega), \quad \forall \vec{\mathbf{v}} \in \mathbf{V}, \quad (3.20)$$

and

$$\tilde{a}_j(\vec{\psi}, \vec{\psi}) \geq \tilde{\alpha} \|\vec{\psi}\|^2 \quad \forall \vec{\psi} \in \tilde{\mathbf{V}}. \quad (3.21)$$

Proof. Given $\vec{\mathbf{v}} = (\mathbf{v}, \mathbf{s}) \in \mathbf{V}$ and $\phi \in \mathbf{L}^4(\Omega)$, we know from (3.14) that $\nabla \mathbf{v} = \mathbf{s}$ and $\mathbf{v} \in \mathbf{H}_0^1(\Omega)$, which yields $\mathbf{e}(\mathbf{v}) = \mathbf{s}_{\operatorname{sym}}$. Hence, applying the lower bound of μ (cf. (2.2)), the Korn inequality in

$\mathbf{H}_0^1(\Omega)$, the continuous injection $\mathbf{i} : \mathbf{H}^1(\Omega) \rightarrow \mathbf{L}^4(\Omega)$, and the Friedrichs–Poincaré inequality with constant c_p , we obtain

$$\begin{aligned} a_\phi(\vec{\mathbf{v}}, \vec{\mathbf{v}}) &= \int_\Omega \gamma \mathbf{v} \cdot \mathbf{v} + \int_\Omega 2\mu(\phi) \mathbf{s}_{sym} : \mathbf{s}_{sym} \geq 2\mu_1 \|\mathbf{s}_{sym}\|_{0,\Omega}^2 = 2\mu_1 \|\mathbf{e}(\mathbf{v})\|_{0,\Omega}^2 \\ &\geq \mu_1 |\mathbf{v}|_{1,\Omega}^2 = \frac{\mu_1}{2} |\mathbf{v}|_{1,\Omega}^2 + \frac{\mu_1}{2} \|\mathbf{s}\|_{0,\Omega}^2 \geq \frac{\mu_1 c_p}{2 \|\mathbf{i}\|^2} \|\mathbf{v}\|_{0,4;\Omega}^2 + \frac{\mu_1}{2} \|\mathbf{s}\|_{0,\Omega}^2, \end{aligned}$$

which implies (3.20) with α depending on μ_1 , c_p , and $\|\mathbf{i}\|$. The proof of (3.21), using that \mathbb{K}_j is a uniformly positive definite tensor, and proceeding analogously to the one of (3.20), is omitted. \blacksquare

We find it important to remark that the \mathbf{V} -ellipticity of a_ϕ does not depend on γ . This property will remain valid for the discrete case, and therefore this constant could be chosen arbitrarily small. In particular, while γ is related to Darcy’s number, it could also arise from time discretization of the evolutionary problem. In this case, and since the aforementioned ellipticity is already guaranteed by the second term defining a_ϕ and by the lower bound μ_1 of μ , we stress that this property will not be affected by a small value of γ , which confirms the relevance of extending the applicability of the theory from [22] to the present model. Next, we recall from [22] that b and \tilde{b} (cf. (3.7) and (3.9)) verify the inf-sup condition corresponding to the Banach version of the Babuška–Brezzi theory.

Lemma 3.2. *There exist positive constants β and $\tilde{\beta}$ such that*

$$\sup_{\substack{\vec{\mathbf{v}} \in \mathbf{H} \\ \vec{\mathbf{v}} \neq 0}} \frac{b(\vec{\mathbf{v}}, \boldsymbol{\tau})}{\|\vec{\mathbf{v}}\|} \geq \beta \|\boldsymbol{\tau}\|_{\mathbf{div}_{4/3};\Omega} \quad \forall \boldsymbol{\tau} \in \mathbb{H}_0(\mathbf{div}_{4/3};\Omega),$$

and

$$\sup_{\substack{\vec{\boldsymbol{\psi}} \in \tilde{\mathbf{H}} \\ \vec{\boldsymbol{\psi}} \neq 0}} \frac{\tilde{b}(\vec{\boldsymbol{\psi}}, \tilde{\boldsymbol{\tau}})}{\|\vec{\boldsymbol{\psi}}\|} \geq \tilde{\beta} \|\tilde{\boldsymbol{\tau}}\|_{\mathbf{div}_{4/3};\Omega} \quad \forall \tilde{\boldsymbol{\tau}} \in \mathbf{H}(\mathbf{div}_{4/3};\Omega).$$

Proof. See [22, Lemma 3.3]. \blacksquare

Furthermore, in what follows we collect also from [22] various fundamental properties of the forms $c(\mathbf{w}; \cdot, \cdot)$ and \tilde{c}_w that are instrumental for the forthcoming analysis.

Lemma 3.3. *The bilinear forms $c(\mathbf{w}; \cdot, \cdot) : \mathbf{H} \times \mathbf{H} \rightarrow \mathbb{R}$ and $\tilde{c}_w : \tilde{\mathbf{H}} \times \tilde{\mathbf{H}} \rightarrow \mathbb{R}$ are bounded for each $\mathbf{w} \in \mathbf{L}^4(\Omega)$ with boundedness constants given in both cases by $\|\mathbf{w}\|_{0,4;\Omega}$. Moreover:*

$$c(\mathbf{w}; \vec{\mathbf{v}}, \vec{\mathbf{v}}) = 0 \quad \text{and} \quad \tilde{c}_w(\vec{\boldsymbol{\varphi}}_j, \vec{\boldsymbol{\varphi}}_j) = 0 \quad \forall \mathbf{w} \in \mathbf{L}^4(\Omega), \quad \forall \vec{\mathbf{v}} \in \mathbf{H}, \quad \forall \vec{\boldsymbol{\varphi}}_j \in \tilde{\mathbf{H}}, \quad (3.22)$$

$$|c(\mathbf{w}; \vec{\mathbf{u}}, \vec{\mathbf{v}}) - c(\mathbf{z}; \vec{\mathbf{u}}, \vec{\mathbf{v}})| \leq \|\mathbf{w} - \mathbf{z}\|_{0,4;\Omega} \|\vec{\mathbf{u}}\| \|\vec{\mathbf{v}}\| \quad \forall \mathbf{w}, \mathbf{z} \in \mathbf{L}^4(\Omega), \quad \forall \vec{\mathbf{u}}, \vec{\mathbf{v}} \in \mathbf{H}, \quad (3.23)$$

$$|\tilde{c}_w(\vec{\boldsymbol{\phi}}_j, \vec{\boldsymbol{\psi}}_j) - \tilde{c}_w(\vec{\boldsymbol{\varphi}}_j, \vec{\boldsymbol{\psi}}_j)| \leq \|\mathbf{w}\|_{0,4;\Omega} \|\vec{\boldsymbol{\phi}}_j - \vec{\boldsymbol{\varphi}}_j\| \|\vec{\boldsymbol{\psi}}_j\| \quad \forall \mathbf{w} \in \mathbf{L}^4(\Omega), \quad \forall \vec{\boldsymbol{\phi}}_j, \vec{\boldsymbol{\varphi}}_j, \vec{\boldsymbol{\psi}}_j \in \tilde{\mathbf{H}}, \quad (3.24)$$

$$|\tilde{c}_w(\vec{\boldsymbol{\varphi}}_j, \vec{\boldsymbol{\psi}}_j) - \tilde{c}_z(\vec{\boldsymbol{\varphi}}_j, \vec{\boldsymbol{\psi}}_j)| \leq \|\mathbf{w} - \mathbf{z}\|_{0,4;\Omega} \|\vec{\boldsymbol{\varphi}}_j\| \|\vec{\boldsymbol{\psi}}_j\| \quad \forall \mathbf{w}, \mathbf{z} \in \mathbf{L}^4(\Omega), \quad \forall \vec{\boldsymbol{\varphi}}_j, \vec{\boldsymbol{\psi}}_j \in \tilde{\mathbf{H}}. \quad (3.25)$$

Proof. See [22, Lemma 3.4]. \blacksquare

Given $(\mathbf{w}, \phi) \in \mathbf{L}^4(\Omega) \times \mathbf{L}^4(\Omega)$, we adopt a similar notation as in [22, Lemma 3.5, 3.6] and introduce the bilinear forms $\mathcal{A}_{\mathbf{w}, \phi} : \mathbf{H} \times \mathbf{H} \rightarrow \mathbb{R}$ and $\tilde{\mathcal{A}}_{\mathbf{w}, j} : \tilde{\mathbf{H}} \times \tilde{\mathbf{H}} \rightarrow \mathbb{R}$ defined by

$$\mathcal{A}_{\mathbf{w}, \phi}(\vec{\mathbf{u}}, \vec{\mathbf{v}}) := a_\phi(\vec{\mathbf{u}}, \vec{\mathbf{v}}) + c(\mathbf{w}, \vec{\mathbf{u}}, \vec{\mathbf{v}}) \quad \forall \vec{\mathbf{u}}, \vec{\mathbf{v}} \in \mathbf{H} \quad (3.26)$$

$$\tilde{\mathcal{A}}_{\mathbf{w}, j}(\vec{\varphi}_j, \vec{\psi}_j) := \tilde{a}_j(\vec{\varphi}_j, \vec{\psi}_j) + c_{\mathbf{w}}(\vec{\varphi}_j, \vec{\psi}_j) \quad \forall \vec{\varphi}_j, \vec{\psi}_j \in \tilde{\mathbf{H}}, \quad (3.27)$$

which, thanks to (3.16), (3.18) and Lemma 3.3, satisfy

$$|\mathcal{A}_{\mathbf{w}, \phi}(\vec{\mathbf{u}}, \vec{\mathbf{v}})| \leq (|\Omega|^{1/2} \gamma + 2\mu_2 + \|\mathbf{w}\|_{0,4;\Omega}) \|\vec{\mathbf{u}}\| \|\vec{\mathbf{v}}\| \quad \forall \vec{\mathbf{u}}, \vec{\mathbf{v}} \in \mathbf{H}, \quad (3.28)$$

$$|\tilde{\mathcal{A}}_{\mathbf{w}, j}(\vec{\varphi}_j, \vec{\psi}_j)| \leq (\|\mathbb{K}_j\|_{0,\infty;\Omega} + \|\mathbf{w}\|_{0,4;\Omega}) \|\vec{\varphi}_j\| \|\vec{\psi}_j\| \quad \forall \vec{\varphi}_j, \vec{\psi}_j \in \tilde{\mathbf{H}}. \quad (3.29)$$

In addition, in virtue of Lemma 3.1 and (3.22), we readily see that $\mathcal{A}_{\mathbf{w}, \phi}$ and $\tilde{\mathcal{A}}_{\mathbf{w}, j}$ are \mathbf{V} -elliptic and $\tilde{\mathbf{V}}$ -elliptic, respectively, with the same constants α and $\tilde{\alpha}$ from Lemma 3.1. According to these results and the inf-sup conditions satisfied by b and \tilde{b} (cf. Lemma 3.2), straightforward applications of the Babuška–Brezzi theory in Banach spaces imply that (3.11) and (3.12) are well-posed, equivalently that the operators S and \tilde{S}_j , $j \in \{1, 2\}$ (and hence \tilde{S}), are all well-defined. More precisely, denoting $\|\mathbb{K}\|_{0,\infty;\Omega} := \|\mathbb{K}_1\|_{0,\infty;\Omega} + \|\mathbb{K}_2\|_{0,\infty;\Omega}$, we are now in position to state the following lemmas.

Lemma 3.4. *For each $(\mathbf{w}, \phi) \in \mathbf{L}^4(\Omega) \times \mathbf{L}^4(\Omega)$, problem (3.11) has a unique solution $(\vec{\mathbf{u}}, \boldsymbol{\sigma}) := ((\mathbf{u}, \mathbf{t}), \boldsymbol{\sigma}) \in \mathbf{H} \times \mathbb{H}_0(\operatorname{div}_{4/3}; \Omega)$. Moreover, there exists $C_S > 0$, independent of (\mathbf{w}, ϕ) , such that*

$$\|S(\mathbf{w}, \phi)\| := \|\mathbf{u}\|_{0,4;\Omega} \leq C_S \left\{ \|\phi\|_{0,4;\Omega} \|\mathbf{g}\|_{0,\infty;\Omega} + (1 + \|\mathbf{w}\|_{0,4;\Omega}) \|\mathbf{u}_D\|_{1/2,\Gamma} \right\}. \quad (3.30)$$

Lemma 3.5. *For each $\mathbf{w} \in \mathbf{L}^4(\Omega)$, and $j \in \{1, 2\}$, problem (3.12) has a unique solution $(\vec{\varphi}_j, \tilde{\boldsymbol{\sigma}}_j) := ((\varphi_j, \tilde{\mathbf{t}}_j), \tilde{\boldsymbol{\sigma}}_j) \in \tilde{\mathbf{H}} \times \mathbf{H}(\operatorname{div}_{4/3}; \Omega)$. Moreover, there exists $C_{\tilde{S}} > 0$, independent of \mathbf{w} , such that*

$$\|\tilde{S}(\mathbf{w})\| := \|(\tilde{S}_1(\mathbf{w}), \tilde{S}_2(\mathbf{w}))\| = \|(\varphi_1, \varphi_2)\| \leq C_{\tilde{S}} \left\{ 1 + \|\mathbb{K}\|_{0,\infty;\Omega} + \|\mathbf{w}\|_{0,4;\Omega} \right\} \|\varphi_D\|_{1/2,\Gamma}. \quad (3.31)$$

We refer to [22, Lemmas 3.5 and 3.6] for similar algebraic details on the a priori estimates (3.30) and (3.31), as well as for the explicit expressions for the constants C_S and $C_{\tilde{S}}$.

3.4. Solvability of the fixed-point equation

Having proved that the operators S , \tilde{S} , and hence T , are well-defined, we now follow [22] to establish the existence of a unique fixed point for T . For sake of simplicity of the remaining analysis, we consider a constant viscosity, but should μ depend on φ , we would only need to assume further regularity on the solution of the problem defining S , exactly as we did in [22, Section 3.4]. In any case, the most distinctive aspects of our subsequent mathematical discussion will remain unchanged.

We begin by observing from (3.13), the a priori bounds for \tilde{S} (cf. Lemma 3.5) and S (cf. Lemma 3.4), and some algebraic manipulations, that for all $(\mathbf{w}, \phi) \in \mathbf{L}^4(\Omega) \times \mathbf{L}^4(\Omega)$ there holds

$$\begin{aligned} \|T(\mathbf{w}, \phi)\| &:= \|(S(\mathbf{w}, \phi), \tilde{S}(S(\mathbf{w}, \phi)))\| = \|S(\mathbf{w}, \phi)\| + \|\tilde{S}(S(\mathbf{w}, \phi))\| \\ &\leq (1 + C_{\tilde{S}} \|\varphi_D\|_{1/2,\Gamma}) \|S(\mathbf{w}, \phi)\| + C_{\tilde{S}} (1 + \|\mathbb{K}\|_{0,\infty;\Omega}) \|\varphi_D\|_{1/2,\Gamma} \\ &\leq C_S \max\{1, C_{\tilde{S}}\} (1 + \|\varphi_D\|_{1/2,\Gamma}) (\|\mathbf{g}\|_{0,\infty;\Omega} + \|\mathbf{u}_D\|_{1/2,\Gamma}) (1 + \|(\mathbf{w}, \phi)\|) \\ &\quad + C_{\tilde{S}} (1 + \|\mathbb{K}\|_{0,\infty;\Omega}) \|\varphi_D\|_{1/2,\Gamma}, \end{aligned} \quad (3.32)$$

from which, assuming that $\|(\mathbf{w}, \phi)\| \leq r$, with $r > 0$ given, we get

$$\|T(\mathbf{w}, \phi)\| \leq C(r) \left\{ (1 + \|\varphi_D\|_{1/2,\Gamma}) (\|\mathbf{g}\|_{0,\infty;\Omega} + \|\mathbf{u}_D\|_{1/2,\Gamma}) + (1 + \|\mathbb{K}\|_{0,\infty;\Omega}) \|\varphi_D\|_{1/2,\Gamma} \right\}, \quad (3.33)$$

with $C(r) := C_S \max\{1, C_{\tilde{S}}\}(r+1) + C_{\tilde{S}}$. In this way, denoting by W the closed ball of $\mathbf{L}^4(\Omega) \times \mathbf{L}^4(\Omega)$ with radius r , we conclude from the foregoing estimate that if the data satisfy the assumption

$$\left\{ (1 + \|\boldsymbol{\varphi}_D\|_{1/2,\Gamma}) (\|\mathbf{g}\|_{0,\infty;\Omega} + \|\mathbf{u}_D\|_{1/2,\Gamma}) + (1 + \|\mathbb{K}\|_{0,\infty;\Omega}) \|\boldsymbol{\varphi}_D\|_{1/2,\Gamma} \right\} \leq \frac{r}{C(r)}, \quad (3.34)$$

then the operator T maps W into itself.

In the following lemmas we establish the continuity of the operators S and \tilde{S} .

Lemma 3.6. *Let α be the \mathbf{V} -ellipticity constant provided by Lemma 3.1 and let $L_S := \alpha^{-1}$. Then*

$$\|S(\mathbf{w}, \boldsymbol{\phi}) - S(\mathbf{z}, \boldsymbol{\psi})\| \leq L_S \left\{ \|\mathbf{w} - \mathbf{z}\|_{0,4;\Omega} \|S(\mathbf{z}, \boldsymbol{\psi})\| + \|\boldsymbol{\phi} - \boldsymbol{\psi}\|_{0,4;\Omega} \|\mathbf{g}\|_{0,\infty;\Omega} \right\}, \quad (3.35)$$

for all $(\mathbf{w}, \boldsymbol{\phi}), (\mathbf{z}, \boldsymbol{\psi}) \in \mathbf{L}^4(\Omega) \times \mathbf{L}^4(\Omega)$.

Proof. It proceeds similarly as in [22, Lemma 3.8 and eq. (3.64)]. We omit further details. \blacksquare

Lemma 3.7. *There exists a positive constant $L_{\tilde{S}}$, depending on $\tilde{\alpha}$ and $C_{\tilde{S}}$ (cf. Lemma 3.5), such that*

$$\|\tilde{S}(\mathbf{w}) - \tilde{S}(\mathbf{z})\| \leq L_{\tilde{S}} \|\mathbf{z} - \mathbf{w}\|_{0,4;\Omega} \left\{ (1 + \|\mathbb{K}\|_{0,\infty;\Omega}) \|\boldsymbol{\varphi}_D\|_{1/2,\Gamma} + \|\mathbf{z}\|_{0,4;\Omega} \|\boldsymbol{\varphi}_D\|_{1/2,\Gamma} \right\}, \quad (3.36)$$

for all $\mathbf{w}, \mathbf{z} \in \mathbf{L}^4(\Omega)$.

Proof. Given $\mathbf{w}, \mathbf{z} \in \mathbf{L}^4(\Omega)$, it suffices to recall that $\tilde{S}(\mathbf{w}) - \tilde{S}(\mathbf{z}) = (\tilde{S}_1(\mathbf{w}) - \tilde{S}_1(\mathbf{z}), \tilde{S}_2(\mathbf{w}) - \tilde{S}_2(\mathbf{z}))$, and then apply the continuity for each \tilde{S}_j , $j \in \{1, 2\}$, provided by [22, Lemma 3.9]. \blacksquare

We are now in a position to establish the continuity of T as a consequence of Lemmas 3.6 and 3.7.

Lemma 3.8. *There holds*

$$\begin{aligned} \|T(\mathbf{w}, \boldsymbol{\phi}) - T(\mathbf{z}, \boldsymbol{\psi})\| &\leq L_S \left\{ 1 + L_{\tilde{S}} \left(1 + \|\mathbb{K}\|_{0,\infty;\Omega} + \|S(\mathbf{z}, \boldsymbol{\psi})\| \right) \|\boldsymbol{\varphi}_D\|_{1/2,\Gamma} \right\} \\ &\quad \times \left\{ \|S(\mathbf{z}, \boldsymbol{\psi})\| + \|\mathbf{g}\|_{0,\infty;\Omega} \right\} \|(\mathbf{w}, \boldsymbol{\phi}) - (\mathbf{z}, \boldsymbol{\psi})\| \end{aligned} \quad (3.37)$$

for all $(\mathbf{w}, \boldsymbol{\phi}), (\mathbf{z}, \boldsymbol{\psi}) \in \mathbf{L}^4(\Omega) \times \mathbf{L}^4(\Omega)$.

Proof. According to the definition of T (cf. (3.13)), and employing the continuity estimate (3.36) for \tilde{S} (cf. Lemma 3.7), we readily find first that

$$\begin{aligned} \|T(\mathbf{w}, \boldsymbol{\phi}) - T(\mathbf{z}, \boldsymbol{\psi})\| &= \|S(\mathbf{w}, \boldsymbol{\phi}) - S(\mathbf{z}, \boldsymbol{\psi})\| + \|\tilde{S}(S(\mathbf{w}, \boldsymbol{\phi})) - \tilde{S}(S(\mathbf{z}, \boldsymbol{\psi}))\| \\ &\leq \left\{ 1 + L_{\tilde{S}} \left(1 + \|\mathbb{K}\|_{0,\infty;\Omega} + \|S(\mathbf{z}, \boldsymbol{\psi})\| \right) \|\boldsymbol{\varphi}_D\|_{1/2,\Gamma} \right\} \|S(\mathbf{w}, \boldsymbol{\phi}) - S(\mathbf{z}, \boldsymbol{\psi})\|, \end{aligned}$$

from which, appealing to the continuity estimate (3.35) for S (Lemma 3.6), we conclude the proof. \blacksquare

Next, given $(\mathbf{z}, \boldsymbol{\psi}) \in \mathbf{L}^4(\Omega) \times \mathbf{L}^4(\Omega)$ such that $\|(\mathbf{z}, \boldsymbol{\psi})\| \leq r$, with $r > 0$ given, we deduce from the a priori estimate (3.30) for S (cf. 3.4) that

$$\|S(\mathbf{z}, \boldsymbol{\psi})\| \leq C_S(1+r) \left\{ \|\mathbf{g}\|_{0,\infty;\Omega} + \|\mathbf{u}_D\|_{1/2,\Gamma} \right\}.$$

In this way, inserting the foregoing estimate back into (3.37), and performing several suitable inequalities, we are able to show the Lipschitz-continuity of T , that is

$$\|T(\mathbf{w}, \boldsymbol{\phi}) - T(\mathbf{z}, \boldsymbol{\psi})\| \leq L_T(1+r)^2 C(\mathbb{K}, \mathbf{g}, \mathbf{u}_D, \boldsymbol{\varphi}_D) \left(\|\mathbf{g}\|_{0,\infty;\Omega} + \|\mathbf{u}_D\|_{1/2,\Gamma} \right) \|(\mathbf{w}, \boldsymbol{\phi}) - (\mathbf{z}, \boldsymbol{\psi})\|, \quad (3.38)$$

for all $(\mathbf{w}, \phi) \in \mathbf{L}^4(\Omega) \times \mathbf{L}^4(\Omega)$, where $L_T := L_S \max\{1, L_{\tilde{S}}\} (\max\{1, C_S\})^2$, and

$$C(\mathbb{K}, \mathbf{g}, \mathbf{u}_D, \varphi_D) := \left\{ 1 + \left(1 + \|\mathbb{K}\|_{0,\infty;\Omega} + \|\mathbf{g}\|_{0,\infty;\Omega} + \|\mathbf{u}_D\|_{1/2,\Gamma} \right) \|\varphi_D\|_{1/2,\Gamma} \right\}. \quad (3.39)$$

We now establish sufficient conditions for the existence of a unique fixed point of T (equivalently, for the well-posedness of the coupled problem (3.6)). More precisely, we have the following result.

Theorem 3.9. *Given $r > 0$, let W be the closed ball in $\mathbf{L}^4(\Omega) \times \mathbf{L}^4(\Omega)$ with center at the origin and radius r , and assume that the data satisfy (3.34) and*

$$L_T(1+r)^2 C(\mathbb{K}, \mathbf{g}, \mathbf{u}_D, \varphi_D) \left(\|\mathbf{g}\|_{0,\infty;\Omega} + \|\mathbf{u}_D\|_{1/2,\Gamma} \right) < 1. \quad (3.40)$$

Then, the operator T has a unique fixed point $(\mathbf{u}, \varphi) \in W$. Equivalently, the coupled problem (3.6) has a unique solution $(\vec{\mathbf{u}}, \boldsymbol{\sigma}) \in \mathbf{H} \times \mathbb{H}_0(\operatorname{div}_{4/3}; \Omega)$ and $(\vec{\varphi}_j, \tilde{\boldsymbol{\sigma}}_j) := ((\varphi_j, \tilde{\mathbf{t}}_j), \tilde{\boldsymbol{\sigma}}_j) \in \tilde{\mathbf{H}} \times \mathbf{H}(\operatorname{div}_{4/3}; \Omega)$, $j \in \{1, 2\}$, with $(\mathbf{u}, \varphi) := (\mathbf{u}, (\varphi_1, \varphi_2)) \in W$. Moreover, there exist positive constants C_i , $i \in \{1, 2, \dots, 6\}$, depending on C_S , r , $C_{\tilde{S}}$, $\|\mathbb{K}\|_{0,\infty;\Omega}$, $|\Omega|$, γ , μ_2 , α , ϑ_1 , ϑ_2 , β , $\tilde{\beta}$, and $\tilde{\alpha}_j$, $j \in \{1, 2\}$, such that the following a priori estimates hold

$$\|\vec{\mathbf{u}}\| \leq C_1 \|\mathbf{g}\|_{0,\infty;\Omega} + C_2 \|\mathbf{u}_D\|_{1/2,\Gamma}, \quad (3.41)$$

$$\|\boldsymbol{\sigma}\| \leq C_3 \|\mathbf{g}\|_{0,\infty;\Omega} + C_4 \|\mathbf{u}_D\|_{1/2,\Gamma}, \quad (3.42)$$

$$\|\vec{\varphi}_j\| \leq C_5 \|\varphi_D\|_{1/2,\Gamma}, \quad (3.43)$$

$$\|\tilde{\boldsymbol{\sigma}}_j\| \leq C_6 \|\varphi_D\|_{1/2,\Gamma}. \quad (3.44)$$

Proof. Let us recall from the first part of the present Subsection 3.4 that, under the assumption (3.34), T maps the ball W into itself. Then, thanks to (3.38) and (3.40), a straightforward application of Banach fixed-point theorem implies the existence of a unique fixed point $(\mathbf{u}, \varphi) \in W$ of T . In turn, the estimates (3.41), (3.43), (3.42), and (3.44) follow similarly to the derivation of the a priori estimates [22, eqs. (3.74), (3.75), (3.76) and (3.77), Theorem 3.11]. \blacksquare

3.5. Incorporating isotropic cross-diffusion

In this section we briefly describe a related model to (2.1), which, on one hand is a particular case of that problem, and on the other hand constitutes a slight modification of it. More precisely, the temperature and concentration equations can accommodate cross-diffusion (see, for instance [16]):

$$\begin{aligned} -\operatorname{div}(\mathbb{K}_{11}\nabla\varphi_1 + \mathbb{K}_{12}\nabla\varphi_2) + \mathbf{u} \cdot \nabla\varphi_1 &= 0 & \text{in } \Omega, \\ -\operatorname{div}(\mathbb{K}_{21}\nabla\varphi_1 + \mathbb{K}_{22}\nabla\varphi_2) + \mathbf{u} \cdot \nabla\varphi_2 &= 0 & \text{in } \Omega, \end{aligned} \quad (3.45)$$

Here, the coefficients $\mathbb{K}_{ij} \in L^\infty(\Omega)$, $i, j \in \{1, 2\}$, are appropriate scalar functions that need to satisfy adequate properties so that the equations remain well-defined. Introducing the tensor

$$\mathbb{K} := \begin{pmatrix} \mathbb{K}_{11} & \mathbb{K}_{12} \\ \mathbb{K}_{21} & \mathbb{K}_{22} \end{pmatrix} \in \mathbb{L}^\infty(\Omega), \quad (3.46)$$

we realize that (3.45) can be rewritten as the system

$$\begin{aligned} -\operatorname{div}(\mathbb{K}\nabla\varphi) + (\nabla\varphi)\mathbf{u} &= 0 & \text{in } \Omega, \\ \varphi &= (\varphi_{1,D}, \varphi_{2,D}) & \text{on } \Gamma, \end{aligned} \quad (3.47)$$

including the Dirichlet boundary conditions for the vector temperature-concentration. In this way, proceeding as in Sections 2 and 3.1, but instead of (2.7), setting

$$\tilde{\mathbf{t}} := \nabla \varphi \quad \text{and} \quad \tilde{\boldsymbol{\sigma}} := \mathbb{K} \tilde{\mathbf{t}} - \frac{1}{2} \varphi \otimes \mathbf{u},$$

we arrive at the following variational formulation for the coupling of (3.47) with the momentum and mass balance equations: Find $(\vec{\mathbf{u}}, \boldsymbol{\sigma}) := ((\mathbf{u}, \mathbf{t}), \boldsymbol{\sigma}) \in (\mathbf{L}^4(\Omega) \times \mathbb{L}_{\text{tr}}^2(\Omega)) \times \mathbb{H}_0(\mathbf{div}_{4/3}; \Omega)$ and $(\vec{\varphi}, \tilde{\boldsymbol{\sigma}}) := ((\varphi, \tilde{\mathbf{t}}), \tilde{\boldsymbol{\sigma}}) \in (\mathbf{L}^4(\Omega) \times \mathbb{L}^2(\Omega)) \times \mathbb{H}(\mathbf{div}_{4/3}; \Omega)$ such that

$$\begin{aligned} a_\varphi(\vec{\mathbf{u}}, \vec{\mathbf{v}}) + c(\mathbf{u}; \vec{\mathbf{u}}, \vec{\mathbf{v}}) + b(\vec{\mathbf{v}}, \boldsymbol{\sigma}) &= F_\varphi(\vec{\mathbf{v}}) \quad \forall \vec{\mathbf{v}} \in (\mathbf{L}^4(\Omega) \times \mathbb{L}_{\text{tr}}^2(\Omega)), \\ b(\vec{\mathbf{u}}, \boldsymbol{\tau}) &= G(\boldsymbol{\tau}) \quad \forall \boldsymbol{\tau} \in \mathbb{H}_0(\mathbf{div}_{4/3}; \Omega), \\ \tilde{a}(\vec{\varphi}, \vec{\boldsymbol{\psi}}) + \tilde{c}_\mathbf{u}(\vec{\varphi}, \vec{\boldsymbol{\psi}}) + \tilde{b}(\vec{\boldsymbol{\psi}}, \tilde{\boldsymbol{\sigma}}) &= 0 \quad \forall \vec{\boldsymbol{\psi}} \in (\mathbf{L}^4(\Omega) \times \mathbb{L}^2(\Omega)), \\ \tilde{b}(\vec{\varphi}, \tilde{\boldsymbol{\tau}}) &= \tilde{G}(\tilde{\boldsymbol{\tau}}) \quad \forall \tilde{\boldsymbol{\tau}} \in \mathbb{H}(\mathbf{div}_{4/3}; \Omega), \end{aligned} \tag{3.48}$$

where, for a given $(\mathbf{w}, \phi) \in \mathbf{L}^4(\Omega) \times \mathbf{L}^4(\Omega)$, the forms a_ϕ , b , and $c(\mathbf{w}; \cdot, \cdot)$, and the functionals F_ϕ and G , are defined as in (3.7),(3.8),(3.10), whereas \tilde{a} , \tilde{b} , $\tilde{c}_\mathbf{w}$, and \tilde{G} , are specified as

$$\begin{aligned} \tilde{a}(\vec{\varphi}, \vec{\boldsymbol{\psi}}) &:= \int_\Omega \mathbb{K} \tilde{\mathbf{t}} : \tilde{\mathbf{s}}, \quad \tilde{b}(\vec{\boldsymbol{\psi}}, \tilde{\boldsymbol{\tau}}) := - \int_\Omega \tilde{\boldsymbol{\tau}} : \tilde{\mathbf{s}} - \int_\Omega \boldsymbol{\psi} \cdot \mathbf{div}(\tilde{\boldsymbol{\tau}}), \\ \tilde{c}_\mathbf{w}(\vec{\varphi}, \vec{\boldsymbol{\psi}}) &:= \frac{1}{2} \left\{ \int_\Omega \tilde{\mathbf{t}} \mathbf{w} \cdot \boldsymbol{\psi} - \int_\Omega (\varphi \otimes \mathbf{w}) : \tilde{\mathbf{s}} \right\}, \quad \tilde{G}(\tilde{\boldsymbol{\tau}}) := - \langle \tilde{\boldsymbol{\tau}} \nu, \varphi_D \rangle_\Gamma, \end{aligned}$$

for all $\vec{\varphi} := (\varphi, \tilde{\mathbf{t}})$, $\vec{\boldsymbol{\psi}} := (\boldsymbol{\psi}, \tilde{\mathbf{s}}) \in \mathbf{L}^4(\Omega) \times \mathbb{L}^2(\Omega)$, for all $\tilde{\boldsymbol{\tau}} \in \mathbb{H}(\mathbf{div}_{4/3}; \Omega)$. Note that the well-posedness analysis for (3.48) follows almost verbatim to that in Sections 3.2–3.5 with a single $j \in \{1, 2\}$ in (3.6), upon the assumption that \mathbb{K} (cf. (3.46)) is uniformly positive definite. We omit further details. A numerical example illustrating the performance of the finite element scheme associated with (3.48) is reported in Section 7.

4. The Galerkin scheme

We now devote ourselves to constructing a Galerkin method for (3.6). The solvability of this scheme is addressed following similar techniques as those employed throughout Section 3.

4.1. Preliminaries

Let us consider arbitrary finite dimensional subspaces $\mathbf{H}_h^\mathbf{u} \subseteq \mathbf{L}^4(\Omega)$, $\mathbb{H}_h^\mathbf{t} \subseteq \mathbb{L}_{\text{tr}}^2(\Omega)$, $\mathbb{H}_h^\boldsymbol{\sigma} \subseteq \mathbb{H}_0(\mathbf{div}_{4/3}; \Omega)$, $\mathbf{H}_h^\varphi \subseteq \mathbf{L}^4(\Omega)$, $\mathbf{H}_h^{\tilde{\mathbf{t}}} \subseteq \mathbb{L}^2(\Omega)$, and $\mathbf{H}_h^{\tilde{\boldsymbol{\sigma}}} \subseteq \mathbf{H}(\mathbf{div}_{4/3}; \Omega)$, whose specific choices are postponed to Section 4.3, below. Hereafter, $h := \max \{h_K : K \in \mathcal{T}_h\}$ stands for the size of a regular triangulation \mathcal{T}_h of $\bar{\Omega}$ formed by triangles K (when $n = 2$) or tetrahedra K (when $n = 3$) of diameter h_K . Next, we denote

$$\begin{aligned} \vec{\mathbf{u}}_h &:= (\mathbf{u}_h, \mathbf{t}_h), \quad \vec{\mathbf{v}}_h := (\mathbf{v}_h, \mathbf{s}_h), \quad \vec{\mathbf{u}}_{0,h} := (\mathbf{u}_{0,h}, \mathbf{t}_{0,h}) \in \mathbf{H}_h := \mathbf{H}_h^\mathbf{u} \times \mathbb{H}_h^\mathbf{t}, \\ \vec{\varphi}_{j,h} &:= (\varphi_{j,h}, \tilde{\mathbf{t}}_{j,h}), \quad \vec{\boldsymbol{\psi}}_{j,h} := (\boldsymbol{\psi}_{j,h}, \tilde{\mathbf{s}}_{j,h}) \in \tilde{\mathbf{H}}_h := \mathbf{H}_h^\varphi \times \mathbf{H}_h^{\tilde{\mathbf{t}}}. \end{aligned}$$

The Galerkin scheme associated with (3.6) reads: Find $(\vec{\mathbf{u}}_h, \boldsymbol{\sigma}_h) \in \mathbf{H}_h \times \mathbb{H}_h^\sigma$ and $(\vec{\boldsymbol{\varphi}}_{j,h}, \vec{\boldsymbol{\sigma}}_{j,h}) \in \tilde{\mathbf{H}}_h \times \mathbf{H}_h^{\tilde{\sigma}}$, $j \in \{1, 2\}$, such that

$$\begin{aligned} a_{\varphi_h}(\vec{\mathbf{u}}_h, \vec{\mathbf{v}}_h) + c(\mathbf{u}_h; \vec{\mathbf{u}}_h, \vec{\mathbf{v}}_h) + b(\vec{\mathbf{v}}_h, \boldsymbol{\sigma}_h) &= F_{\varphi_h}(\vec{\mathbf{v}}_h) \quad \forall \vec{\mathbf{v}}_h \in \mathbf{H}_h, \\ b(\vec{\mathbf{u}}_h, \boldsymbol{\tau}_h) &= G(\boldsymbol{\tau}_h) \quad \forall \boldsymbol{\tau}_h \in \mathbb{H}_h^\sigma, \\ \tilde{a}_j(\vec{\boldsymbol{\varphi}}_{j,h}, \vec{\boldsymbol{\psi}}_{j,h}) + \tilde{c}_{\mathbf{u}_h}(\vec{\boldsymbol{\varphi}}_{j,h}, \vec{\boldsymbol{\psi}}_{j,h}) + \tilde{b}(\vec{\boldsymbol{\psi}}_{j,h}, \vec{\boldsymbol{\sigma}}_{j,h}) &= 0 \quad \forall \vec{\boldsymbol{\psi}}_{j,h} \in \tilde{\mathbf{H}}_h, \\ \tilde{b}(\vec{\boldsymbol{\varphi}}_{j,h}, \vec{\boldsymbol{\tau}}_{j,h}) &= \tilde{G}_j(\vec{\boldsymbol{\tau}}_{j,h}) \quad \forall \vec{\boldsymbol{\tau}}_{j,h} \in \mathbf{H}_h^{\tilde{\sigma}}. \end{aligned} \quad (4.1)$$

We now follow a discrete analogue of the fixed-point approach developed in Section 3.2. To this end, we first let $\mathbf{H}_h^\varphi := \mathbf{H}_h^\varphi \times \mathbf{H}_h^\varphi$ and introduce the operator $S_h : \mathbf{H}_h^\mathbf{u} \times \mathbf{H}_h^\varphi \rightarrow \mathbf{H}_h^\mathbf{u}$ defined by

$$S_h(\mathbf{w}_h, \boldsymbol{\phi}_h) := \mathbf{u}_h \quad \forall (\mathbf{w}_h, \boldsymbol{\phi}_h) \in \mathbf{H}_h^\mathbf{u} \times \mathbf{H}_h^\varphi,$$

where $(\vec{\mathbf{u}}_h, \boldsymbol{\sigma}_h) = ((\mathbf{u}_h, \mathbf{t}_h), \boldsymbol{\sigma}_h) \in \mathbf{H}_h \times \mathbb{H}_h^\sigma$ is the unique solution (to be confirmed below) of the problem

$$\begin{aligned} a_{\phi_h}(\vec{\mathbf{u}}_h, \vec{\mathbf{v}}_h) + c(\mathbf{w}_h; \vec{\mathbf{u}}_h, \vec{\mathbf{v}}_h) + b(\vec{\mathbf{v}}_h, \boldsymbol{\sigma}_h) &= F_{\phi_h}(\vec{\mathbf{v}}_h) \quad \forall \vec{\mathbf{v}}_h \in \mathbf{H}_h, \\ b(\vec{\mathbf{u}}_h, \boldsymbol{\tau}_h) &= G(\boldsymbol{\tau}_h) \quad \forall \boldsymbol{\tau}_h \in \mathbb{H}_h^\sigma. \end{aligned} \quad (4.2)$$

In turn, for each $j \in \{1, 2\}$ we let $\tilde{S}_{j,h} : \mathbf{H}_h^\mathbf{u} \rightarrow \mathbf{H}_h^\varphi$ be the operator given by

$$\tilde{S}_{j,h}(\mathbf{w}_h) := \varphi_{j,h} \quad \forall \mathbf{w}_h \in \mathbf{H}_h^\mathbf{u},$$

where $(\vec{\boldsymbol{\varphi}}_{j,h}, \vec{\boldsymbol{\sigma}}_{j,h}) = ((\varphi_{j,h}, \mathbf{t}_{j,h}), \vec{\boldsymbol{\sigma}}_{j,h}) \in \tilde{\mathbf{H}}_h \times \mathbf{H}_h^{\tilde{\sigma}}$ is the unique solution (to be confirmed below) of the problem

$$\begin{aligned} \tilde{a}_j(\vec{\boldsymbol{\varphi}}_{j,h}, \vec{\boldsymbol{\psi}}_{j,h}) + \tilde{c}_{\mathbf{w}_h}(\vec{\boldsymbol{\varphi}}_{j,h}, \vec{\boldsymbol{\psi}}_{j,h}) + \tilde{b}(\vec{\boldsymbol{\psi}}_{j,h}, \vec{\boldsymbol{\sigma}}_{j,h}) &= 0 \quad \forall \vec{\boldsymbol{\psi}}_{j,h} \in \tilde{\mathbf{H}}_h, \\ \tilde{b}(\vec{\boldsymbol{\varphi}}_{j,h}, \vec{\boldsymbol{\tau}}_{j,h}) &= \tilde{G}_j(\vec{\boldsymbol{\tau}}_{j,h}) \quad \forall \vec{\boldsymbol{\tau}}_{j,h} \in \mathbf{H}_h^{\tilde{\sigma}}, \end{aligned} \quad (4.3)$$

and then we introduce $\tilde{S}_h(\mathbf{w}_h) := (\tilde{S}_{1,h}(\mathbf{w}_h), \tilde{S}_{2,h}(\mathbf{w}_h)) \in \mathbf{H}_h^\varphi$ for all $\mathbf{w}_h \in \mathbf{H}_h^\mathbf{u}$. Hence, defining $T_h : \mathbf{H}_h^\mathbf{u} \times \mathbf{H}_h^\varphi \rightarrow \mathbf{H}_h^\mathbf{u} \times \mathbf{H}_h^\varphi$ as

$$T_h(\mathbf{w}_h, \boldsymbol{\phi}_h) := (S_h(\mathbf{w}_h, \boldsymbol{\phi}_h), \tilde{S}_h(S_h(\mathbf{w}_h, \boldsymbol{\phi}_h))) \quad \forall (\mathbf{w}_h, \boldsymbol{\phi}_h) \in \mathbf{H}_h^\mathbf{u} \times \mathbf{H}_h^\varphi, \quad (4.4)$$

we realize that solving (4.1) is equivalent to seeking a fixed point of T_h , that is: Find $(\mathbf{u}_h, \boldsymbol{\varphi}_h) \in \mathbf{H}_h^\mathbf{u} \times \mathbf{H}_h^\varphi$ such that

$$T_h(\mathbf{u}_h, \boldsymbol{\varphi}_h) = (\mathbf{u}_h, \boldsymbol{\varphi}_h). \quad (4.5)$$

4.2. Solvability of the discrete problem

We now aim to establish the well-posedness of (4.1) by studying the solvability of the equivalent equation (4.5) using Brouwer's fixed-point theorem (cf. [20, Theorem 9.9-2]). Exactly as for the continuous case, we begin by showing that S_h and $\tilde{S}_{j,h}$, $j \in \{1, 2\}$, and hence \tilde{S}_h and T_h , are well-defined. For this purpose, we need to establish hypotheses on the (so far, arbitrary) discrete spaces. Subsequently we will specify suitable finite element spaces satisfying these conditions.

In what follows, we let \mathbf{V}_h and $\tilde{\mathbf{V}}_h$ be the discrete kernels of b and \tilde{b} , respectively, that is

$$\begin{aligned} \mathbf{V}_h &:= \left\{ \vec{\mathbf{v}}_h := (\mathbf{v}_h, \mathbf{s}_h) \in \mathbf{H}_h : \int_{\Omega} \boldsymbol{\tau}_h : \mathbf{s}_h + \int_{\Omega} \mathbf{v}_h \cdot \mathbf{div}(\boldsymbol{\tau}_h) = 0 \quad \forall \boldsymbol{\tau}_h \in \mathbb{H}_h^\sigma \right\}, \\ \tilde{\mathbf{V}}_h &:= \left\{ \vec{\boldsymbol{\psi}}_h := (\boldsymbol{\psi}_h, \tilde{\mathbf{s}}_h) \in \tilde{\mathbf{H}}_h : \int_{\Omega} \tilde{\boldsymbol{\tau}}_h \cdot \tilde{\mathbf{s}}_h + \int_{\Omega} \boldsymbol{\psi}_h \mathbf{div}(\tilde{\boldsymbol{\tau}}_h) = 0 \quad \forall \tilde{\boldsymbol{\tau}}_h \in \mathbf{H}_h^{\tilde{\sigma}} \right\}. \end{aligned}$$

In addition, for each $\mathbf{s}_h \in \mathbb{H}_h^\mathbf{t}$ we denote by $\mathbf{s}_{h,sym}$ and $\mathbf{s}_{h,skw}$ its symmetric and skew-symmetric parts, respectively.

Then, we consider the following hypotheses on the discrete subspaces employed:

Assumption 4.1. *There exists a positive constant $\beta_a > 0$, independent of h , such that*

$$\sup_{\substack{\vec{\mathbf{v}}_h \in \mathbf{H}_h \\ \vec{\mathbf{v}}_h \neq \mathbf{0}}} \frac{b(\vec{\mathbf{v}}_h, \boldsymbol{\tau}_h)}{\|\vec{\mathbf{v}}_h\|} \geq \beta_a \|\boldsymbol{\tau}_h\|_{\text{div}_{4/3}; \Omega} \quad \forall \boldsymbol{\tau}_h \in \mathbb{H}_h^\sigma. \quad (4.6)$$

Assumption 4.2. *There exists a positive constant C_a , independent of h , such that*

$$\|\mathbf{s}_{h, \text{sym}}\|_{0, \Omega} \geq C_a \|(\mathbf{v}_h, \mathbf{s}_{h, \text{skw}})\| \quad \forall \vec{\mathbf{v}}_h := (\mathbf{v}_h, \mathbf{s}_h) \in \mathbf{V}_h. \quad (4.7)$$

Assumption 4.3. *There exists a positive constant $\tilde{\beta}_a > 0$, independent of h , such that*

$$\sup_{\substack{\vec{\boldsymbol{\psi}}_{j,h} \in \tilde{\mathbf{H}}_h \\ \vec{\boldsymbol{\psi}}_{j,h} \neq \mathbf{0}}} \frac{\tilde{b}(\vec{\boldsymbol{\psi}}_{j,h}, \tilde{\boldsymbol{\tau}}_{j,h})}{\|\vec{\boldsymbol{\psi}}_{j,h}\|} \geq \tilde{\beta}_a \|\tilde{\boldsymbol{\tau}}_{j,h}\|_{\text{div}_{4/3}; \Omega} \quad \forall \tilde{\boldsymbol{\tau}}_{j,h} \in \tilde{\mathbf{H}}_h^\sigma. \quad (4.8)$$

Assumption 4.4. *There exists a positive constant \tilde{C}_a , independent of h , such that*

$$\|\tilde{\mathbf{s}}_{j,h}\|_{0, \Omega} \geq \tilde{C}_a \|\boldsymbol{\psi}_{j,h}\|_{0,4; \Omega} \quad \forall \vec{\boldsymbol{\psi}}_{j,h} := (\boldsymbol{\psi}_{j,h}, \tilde{\mathbf{s}}_{j,h}) \in \tilde{\mathbf{V}}_h. \quad (4.9)$$

As consequence of Assumptions 4.1 and 4.2, and following basically the same procedure and notations from [22, Lemma 4.2], we are able to establish next the well-definedness of S_h , which constitutes the discrete analogue of Lemma 3.4.

Lemma 4.5. *For each $(\mathbf{w}_h, \phi_h) \in \mathbf{H}_h^{\mathbf{u}} \times \mathbf{H}_h^\varphi$, (4.2) has a unique solution $(\vec{\mathbf{u}}_h, \boldsymbol{\sigma}_h) := ((\mathbf{u}_h, \mathbf{t}_h), \boldsymbol{\sigma}_h) \in \mathbf{H}_h \times \mathbb{H}_h^\sigma$. Moreover there exists a positive constant $C_{S,a}$, independent of h and (\mathbf{w}_h, ϕ_h) , such that*

$$\|S_h(\mathbf{w}_h, \phi_h)\| := \|\mathbf{u}_h\| \leq C_{S,a} \left\{ \|\phi_h\|_{0,4; \Omega} \|\mathbf{g}\|_{0, \infty; \Omega} + (1 + \|\mathbf{w}_h\|_{0,4; \Omega}) \|\mathbf{u}_D\|_{1/2, \Gamma} \right\}. \quad (4.10)$$

Proof. Given $(\mathbf{w}_h, \phi_h) \in \mathbf{H}_h^{\mathbf{u}} \times \mathbf{H}_h^\varphi$, we first recall from (3.26) and (3.28) that $\mathcal{A}_{\mathbf{w}_h, \phi_h}$ is bounded. Then, for each $\vec{\mathbf{v}}_h := (\mathbf{v}_h, \mathbf{s}_h) \in \mathbf{V}_h$ we easily deduce from (2.2), (4.7) (cf. Assumption 4.2), and a simple algebraic manipulation, that

$$a_{\phi_h}(\vec{\mathbf{v}}_h, \vec{\mathbf{v}}_h) = \int_{\Omega} \gamma \mathbf{v}_h \cdot \mathbf{v}_h + \int_{\Omega} 2\mu(\phi_h) \mathbf{s}_{h, \text{sym}} : \mathbf{s}_{h, \text{sym}} \geq \mu_1 \min\{1, C_a^2\} \|\vec{\mathbf{v}}_h\|^2,$$

which, together with the fact that $c(\mathbf{w}_h; \vec{\mathbf{v}}_h, \vec{\mathbf{v}}_h) = 0 \quad \forall \vec{\mathbf{v}}_h \in \mathbf{H}_h$ (cf. (3.22)), yields the \mathbf{V}_h -ellipticity of both a_{ϕ_h} and $\mathcal{A}_{\mathbf{w}_h, \phi_h}$ with constant $\alpha_a := \mu_1 \min\{1, C_a^2\}$. In turn, it is clear from Assumption 4.1 that b satisfies the discrete inf-sup condition required by the Babuška–Brezzi theorem in Banach spaces. Invoking then that theorem we readily obtain both the unique solvability of (4.2) and the a priori estimate (4.10), with a positive constant $C_{S,a}$ depending on Ω , μ_2 , $\boldsymbol{\vartheta}$, γ , α_a and β_a . \blacksquare

Similarly as we did in the continuous case, we remark that the \mathbf{V}_h -ellipticity of a_{ϕ_h} , and hence of $\mathcal{A}_{\mathbf{w}_h, \phi_h}$, does not depend on γ , certainly yielding the same appealing features mentioned in Section 3.3.

Next, as consequence of Assumptions 4.3 and 4.4, we provide the well-definedness of $\tilde{S}_{j,h}$, $j \in \{1, 2\}$, and hence of \tilde{S}_h , thus establishing the discrete analogue of Lemma 3.5.

Lemma 4.6. *For each $\mathbf{w}_h \in \mathbf{H}_h^{\mathbf{u}}$, and for each $j \in \{1, 2\}$, (4.3) has a unique solution $(\vec{\boldsymbol{\varphi}}_{j,h}, \tilde{\boldsymbol{\sigma}}_{j,h}) := ((\boldsymbol{\varphi}_{j,h}, \tilde{\mathbf{t}}_{j,h}), \tilde{\boldsymbol{\sigma}}_{j,h}) \in \tilde{\mathbf{H}}_h \times \tilde{\mathbf{H}}_h^\sigma$. Moreover, there exists a positive constant $C_{\tilde{S},a}$, independent of h and \mathbf{w}_h , such that*

$$\begin{aligned} \|\tilde{S}_h(\mathbf{w}_h)\| &:= \|(\tilde{S}_{1,h}(\mathbf{w}_h), \tilde{S}_{2,h}(\mathbf{w}_h))\| = \|(\boldsymbol{\varphi}_{1,h}, \boldsymbol{\varphi}_{2,h})\| \\ &\leq C_{\tilde{S},a} \left\{ 1 + \|\mathbb{K}\|_{0, \infty; \Omega} + \|\mathbf{w}_h\|_{0,4; \Omega} \right\} \|\boldsymbol{\varphi}_D\|_{1/2, \Gamma}. \end{aligned} \quad (4.11)$$

Proof. Given $\mathbf{w}_h \in \mathbf{H}_h^{\mathbf{u}}$, we know from (3.27) and (3.29) that each $\tilde{\mathcal{A}}_{\mathbf{w}_h, j}$ is bounded. In addition, it is easy to see, thanks to the uniform positive definiteness of \mathbb{K}_j , the Assumption 4.4, and the fact that $\tilde{c}_{\mathbf{w}_h}(\vec{\varphi}_{j,h}, \vec{\varphi}_{j,h}) = 0 \forall \vec{\varphi}_{j,h} \in \tilde{\mathbf{H}}_h$ (cf. (3.22)), that \tilde{a}_j and $\tilde{\mathcal{A}}_{\mathbf{w}_h, j}$ are $\tilde{\mathbf{V}}_h$ -elliptic with a positive constant $\tilde{\alpha}_{j,d}$. In turn, it is clear from Assumption 4.3 that \tilde{b} satisfies an adequate discrete inf-sup condition and then the Banach version of the Babuška–Brezzi theory implies unique solvability of (4.3) for each $j \in \{1, 2\}$. Moreover, a priori estimates for each $\tilde{S}_{j,h}(\mathbf{w}_h)$ imply (4.11) with a positive constant $C_{\tilde{S},d}$ depending on $\tilde{\alpha}_d$ and $\tilde{\beta}_d$. \blacksquare

Proceeding as in the beginning of Section 3.4 but now for T_h (cf. (4.4)), we employ the a priori bounds (4.10) and (4.11), and denote by W_h the closed ball of $\mathbf{H}_h^{\mathbf{u}} \times \mathbf{H}_h^{\varphi}$ with center at the origin and radius r . We find that for each $(\mathbf{w}_h, \phi_h) \in W_h$ there holds

$$\|T_h(\mathbf{w}_h, \phi_h)\| \leq C_d(r) \left\{ (1 + \|\varphi_D\|_{1/2,\Gamma}) (\|\mathbf{g}\|_{0,\infty;\Omega} + \|\mathbf{u}_D\|_{1/2,\Gamma}) + (1 + \|\mathbb{K}\|_{0,\infty;\Omega}) \|\varphi_D\|_{1/2,\Gamma} \right\},$$

with $C_d(r) := C_{S,d} \max\{1, C_{\tilde{S},d}\}(r+1) + C_{\tilde{S},d}$. It readily follows that, under the assumption

$$\left\{ (1 + \|\varphi_D\|_{1/2,\Gamma}) (\|\mathbf{g}\|_{0,\infty;\Omega} + \|\mathbf{u}_D\|_{1/2,\Gamma}) + (1 + \|\mathbb{K}\|_{0,\infty;\Omega}) \|\varphi_D\|_{1/2,\Gamma} \right\} \leq \frac{r}{C_d(r)}, \quad (4.12)$$

the operator T_h maps W_h into itself.

At this point we remark that, given a radius r , and once $C_d(r)$ is computed according to the above defined expression, the constraint (4.12) is clearly satisfied for sufficiently small $\|\varphi_D\|_{1/2,\Gamma}$, $\|\mathbf{g}\|_{0,\infty;\Omega}$, $\|\mathbf{u}_D\|_{1/2,\Gamma}$, and $\|\mathbb{K}\|_{0,\infty;\Omega}$. However, the dependence of $C_{S,d}$ and $C_{\tilde{S},d}$ (which define $C_d(r)$) on the constants and parameters specified at the end of the proofs of Lemmas 4.5 and 4.6, respectively, and the fact that some of the latter might not be known explicitly, makes it hard to actually verify (4.12) in practice. Indeed, as aforementioned, we are certain that there do exist data satisfying this condition, but, unless all the constants and parameters involved are explicitly known, we do not know how small they are. The same comment applies to other similar constraints along the paper.

In analogy with the continuous case, the continuity of T_h follows from that of S_h , $\tilde{S}_{j,h}$, $j \in \{1, 2\}$, and hence \tilde{S}_h . Proceeding as in [22, Lemmas 4.5 and 4.6], we prove the discrete analogues of Lemmas 3.6 and 3.7. More precisely, there exist positive constants $L_{S,d}$ and $L_{\tilde{S},d}$, both independent of h , the first one given by α_d^{-1} (cf. proof of Lemma 4.5), and the second one depending on $\tilde{\alpha}_d$ and $C_{\tilde{S},d}$ (cf. proof of Lemma 4.6), such that

$$\|S_h(\mathbf{w}_h, \phi_h) - S_h(\mathbf{z}_h, \psi_h)\| \leq L_{S,d} \left\{ \|\mathbf{w}_h - \mathbf{z}_h\|_{0,4;\Omega} \|S_h(\mathbf{z}_h, \psi_h)\| + \|\phi_h - \psi_h\|_{0,4;\Omega} \|\mathbf{g}\|_{0,\infty;\Omega} \right\}, \quad (4.13)$$

for all $(\mathbf{w}_h, \phi_h), (\mathbf{z}_h, \psi_h) \in \mathbf{H}_h^{\mathbf{u}} \times \mathbf{H}_h^{\varphi}$, and

$$\|\tilde{S}_h(\mathbf{w}_h) - \tilde{S}_h(\mathbf{z}_h)\| \leq L_{\tilde{S},d} \|\mathbf{z}_h - \mathbf{w}_h\|_{0,4;\Omega} \left\{ (1 + \|\mathbb{K}\|_{0,\infty;\Omega}) \|\varphi_D\|_{1/2,\Gamma} + \|\mathbf{z}_h\|_{0,4;\Omega} \|\varphi_D\|_{1/2,\Gamma} \right\}, \quad (4.14)$$

for all $\mathbf{w}_h, \mathbf{z}_h \in \mathbf{H}_h^{\mathbf{u}}$. Then, as a straightforward consequence of (4.13) and (4.14), and following the same steps from the second half of Section 3.4, we arrive at the discrete analogue of (3.38), that is

$$\begin{aligned} & \|T_h(\mathbf{w}_h, \phi_h) - T_h(\mathbf{z}_h, \psi_h)\| \\ & \leq L_{T,d} (1+r)^2 C(\mathbb{K}, \mathbf{g}, \mathbf{u}_D, \varphi_D) \left(\|\mathbf{g}\|_{0,\infty;\Omega} + \|\mathbf{u}_D\|_{1/2,\Gamma} \right) \|(\mathbf{w}_h, \phi_h) - (\mathbf{z}_h, \psi_h)\| \end{aligned} \quad (4.15)$$

for all $(\mathbf{w}_h, \phi_h) \in \mathbf{H}_h^{\mathbf{u}} \times \mathbf{H}_h^{\varphi}$, where

$$L_{T,d} := L_{S,d} \max\{1, L_{\tilde{S},d}\} (\max\{1, C_{S,d}\})^2,$$

and $C(\mathbb{K}, \mathbf{g}, \mathbf{u}_D, \varphi_D)$ is given by (3.39).

Then, we are in position to establish our main result.

Theorem 4.7. *Assume that the data satisfy (4.12) and*

$$L_{T,d}(1+r)^2 C(\mathbb{K}, \mathbf{g}, \mathbf{u}_D, \boldsymbol{\varphi}_D) \left(\|\mathbf{g}\|_{0,\infty;\Omega} + \|\mathbf{u}_D\|_{1/2,\Gamma} \right) < 1. \quad (4.16)$$

Then, the operator T_h has a unique fixed point $(\mathbf{u}_h, \boldsymbol{\varphi}_h) \in W_h$. Equivalently, the coupled problem (4.1) has a unique solution $(\vec{\mathbf{u}}_h, \boldsymbol{\sigma}_h) \in \mathbf{H}_h \times \mathbb{H}_h^\sigma$ and $(\vec{\boldsymbol{\varphi}}_{j,h}, \tilde{\boldsymbol{\sigma}}_{j,h}) := ((\varphi_{j,h}, \tilde{\mathbf{t}}_j), \tilde{\boldsymbol{\sigma}}_{j,h}) \in \tilde{\mathbf{H}}_h \times \mathbf{H}_h^\sigma$, $j \in \{1, 2\}$, with $(\mathbf{u}_h, \boldsymbol{\varphi}_h) := (\mathbf{u}_h, (\varphi_{1,h}, \varphi_{2,h})) \in W_h$. Moreover, there exist positive constants $C_{i,d}$, $i \in \{1, 2, \dots, 6\}$, depending on $C_{S,d}$, r , $C_{\tilde{S},d}$, $\|\mathbb{K}\|_{0,\infty;\Omega}$, $|\Omega|$, γ , μ_2 , α_d , ϑ_1 , ϑ_2 , β_d , $\tilde{\beta}_d$, and $\tilde{\alpha}_{j,d}$, $j \in \{1, 2\}$, such that the following a priori estimates hold

$$\|\vec{\mathbf{u}}_h\| \leq C_{1,d} \|\mathbf{g}\|_{0,\infty;\Omega} + C_{2,d} \|\mathbf{u}_D\|_{1/2,\Gamma}, \quad (4.17)$$

$$\|\boldsymbol{\sigma}_h\| \leq C_{3,d} \|\mathbf{g}\|_{0,\infty;\Omega} + C_{4,d} \|\mathbf{u}_D\|_{1/2,\Gamma}, \quad (4.18)$$

$$\|\vec{\boldsymbol{\varphi}}_{j,h}\| \leq C_{5,d} \|\boldsymbol{\varphi}_D\|_{1/2,\Gamma}, \quad (4.19)$$

$$\|\tilde{\boldsymbol{\sigma}}_{j,h}\| \leq C_{6,d} \|\boldsymbol{\varphi}_D\|_{1/2,\Gamma}. \quad (4.20)$$

Proof. We first recall that, under the assumption (4.12), T_h maps W_h into itself. Then, (4.15), (4.16), and the Banach fixed-point theorem conclude the proof. The a priori estimates (4.17), (4.19), (4.18), and (4.20) are derived similarly as for [22, eqs. (4.26)-(4.29), Theorem 4.8]. \blacksquare

We end this section by remarking that if the viscosity depends on temperature and concentration, it is not possible to establish the Lipschitz-continuity of T_h (cf. (4.15)), but just continuity. Consequently, instead of the Banach theorem, the Brouwer fixed-point theorem is applied, thus yielding only existence of the discrete solution. For related details, we refer to [22, Section 4.2].

4.3. Specific finite element subspaces

In this section we specify finite element subspaces $\mathbf{H}_h^{\mathbf{u}} \subseteq \mathbf{L}^4(\Omega)$, $\mathbb{H}_h^{\mathbf{t}} \subseteq \mathbb{L}_{\text{tr}}^2(\Omega)$, $\mathbb{H}_h^\sigma \subseteq \mathbb{H}_0(\mathbf{div}_{4/3}; \Omega)$, $\mathbf{H}_h^\varphi \subseteq \mathbf{L}^4(\Omega)$, $\tilde{\mathbf{H}}_h^{\mathbf{t}} \subseteq \mathbf{L}^2(\Omega)$, and $\tilde{\mathbf{H}}_h^\sigma \subseteq \mathbf{H}(\mathbf{div}_{4/3}; \Omega)$, satisfying the crucial discrete inf-sup conditions given by Assumptions 4.1, 4.2, 4.3, and 4.4. These discrete spaces arise naturally as consequence of the same analysis developed in [22, Section 5], which is based on stable finite element subspaces for the primal formulation of the Stokes problem (see also [12] for the case of linear elasticity). In particular, here we propose those obtained by considering the Scott-Vogelius pair (cf. [45]). Given a positive integer ℓ and a set $\mathcal{O} \subseteq \mathbb{R}^n$, $\mathbf{P}_\ell(\mathcal{O})$ stands for the space of polynomials of degree $\leq \ell$ defined on \mathcal{O} , with vector and tensorial versions denoted by $\mathbf{P}_\ell(\mathcal{O}) := [\mathbf{P}_\ell(\mathcal{O})]^n$ and $\mathbb{P}_\ell(\mathcal{O}) := [\mathbf{P}_\ell(\mathcal{O})]^{n \times n}$, respectively. In addition, given a regular partition \mathcal{T}_h of $\bar{\Omega}$ into triangles (in \mathbb{R}^2) or tetrahedra (in \mathbb{R}^3), we denote by $\mathcal{T}_h^{\mathbf{b}}$ its barycentric refinement, and let $\mathbf{RT}_\ell(K) := \mathbf{P}_\ell(K) \oplus \mathbf{P}_\ell(K)\mathbf{x}$ be the local Raviart–Thomas space of order ℓ for each $K \in \mathcal{T}_h^{\mathbf{b}}$, where \mathbf{x} denotes a generic vector in Ω .

We deduce that, in order to guarantee the well-posedness of our Galerkin scheme (4.1), it suffices to define for each integer k such that $k+1 \geq n$, the finite element subspaces

$$\mathbf{H}_h^{\mathbf{u}} := \left\{ \mathbf{v}_h \in \mathbf{L}^4(\Omega) : \mathbf{v}_h|_K \in \mathbf{P}_k(K) \quad \forall K \in \mathcal{T}_h^{\mathbf{b}} \right\}, \quad (4.21)$$

$$\mathbb{H}_h^{\mathbf{t}} := \left\{ \mathbf{s}_h \in \mathbb{L}_{\text{tr}}^2(\Omega) : \mathbf{s}_h|_K \in \mathbb{P}_k(K) \quad \forall K \in \mathcal{T}_h^{\mathbf{b}} \right\}, \quad (4.22)$$

$$\mathbb{H}_h^\sigma := \left\{ \boldsymbol{\tau}_h \in \mathbb{H}_0(\mathbf{div}_{4/3}; \Omega) : \mathbf{c}^{\mathbf{t}} \boldsymbol{\tau}_h|_K \in \mathbf{RT}_k(K) \quad \forall \mathbf{c} \in \mathbb{R}^n, \quad \forall K \in \mathcal{T}_h^{\mathbf{b}} \right\}, \quad (4.23)$$

$$\mathbf{H}_h^\varphi := \left\{ \psi_h \in \mathbf{L}^4(\Omega) : \psi_h|_K \in \mathbf{P}_k(K) \quad \forall K \in \mathcal{T}_h^{\mathbf{b}} \right\}, \quad (4.24)$$

$$\mathbf{H}_h^{\tilde{\mathbf{t}}} := \left\{ \tilde{\mathbf{s}}_h \in \mathbf{L}^2(\Omega) : \tilde{\mathbf{s}}_h|_K \in \mathbf{P}_k(K) \quad \forall K \in \mathcal{T}_h^{\mathbf{b}} \right\}, \quad (4.25)$$

$$\mathbf{H}_h^{\tilde{\sigma}} := \left\{ \tilde{\boldsymbol{\tau}}_h \in \mathbf{H}(\operatorname{div}_{4/3}; \Omega) : \tilde{\boldsymbol{\tau}}_h|_K \in \mathbf{RT}_k(K) \quad \forall K \in \mathcal{T}_h^{\mathbf{b}} \right\}. \quad (4.26)$$

We end this section by collecting next the approximation properties of the finite element subspaces $\mathbf{H}_h^{\mathbf{u}}$, $\mathbb{H}_h^{\mathbf{t}}$, \mathbb{H}_h^{σ} , \mathbf{H}_h^{φ} , $\mathbf{H}_h^{\tilde{\mathbf{t}}}$, and $\mathbf{H}_h^{\tilde{\sigma}}$, which basically follow from interpolation estimates of Sobolev spaces and the approximation properties provided by the projector \mathcal{P}_h^k (see [22, eq. (5.37)]), and the Raviart–Thomas interpolation operator (see [22, eq. (5.41)] and also [13, 15, 30]).

($\mathbf{AP}_h^{\mathbf{u}}$) there exists $C > 0$, independent of h , such that for each $l \in [0, k+1]$, and for each $\mathbf{v} \in \mathbf{W}^{l,4}(\Omega)$ there holds

$$\operatorname{dist}(\mathbf{v}, \mathbf{H}_h^{\mathbf{u}}) := \inf_{\mathbf{v}_h \in \mathbf{H}_h^{\mathbf{u}}} \|\mathbf{v} - \mathbf{v}_h\|_{0,4;\Omega} \leq Ch^l \|\mathbf{v}\|_{l,4;\Omega}. \quad (4.27)$$

($\mathbf{AP}_h^{\mathbf{t}}$) there exists $C > 0$, independent of h , such that for each $l \in [0, k+1]$, and for each $\mathbf{s} \in \mathbb{H}^l(\Omega) \cap \mathbb{L}_{\operatorname{tr}}^2(\Omega)$ there holds

$$\operatorname{dist}(\mathbf{s}, \mathbb{H}_h^{\mathbf{t}}) := \inf_{\mathbf{s}_h \in \mathbb{H}_h^{\mathbf{t}}} \|\mathbf{s} - \mathbf{s}_h\|_{0,\Omega} \leq Ch^l \|\mathbf{s}\|_{l,\Omega}. \quad (4.28)$$

(\mathbf{AP}_h^{σ}) there exists $C > 0$, independent of h , such that for each $l \in [0, k+1]$, and for each $\boldsymbol{\tau} \in \mathbb{H}^l(\Omega) \cap \mathbb{H}_0(\operatorname{div}_{4/3}; \Omega)$ with $\operatorname{div}(\boldsymbol{\tau}) \in \mathbf{W}^{l,4/3}(\Omega)$, there holds

$$\operatorname{dist}(\boldsymbol{\tau}, \mathbb{H}_h^{\sigma}) := \inf_{\boldsymbol{\tau}_h \in \mathbb{H}_h^{\sigma}} \|\boldsymbol{\tau} - \boldsymbol{\tau}_h\|_{\operatorname{div}_{4/3};\Omega} \leq Ch^l \left\{ \|\boldsymbol{\tau}\|_{l,\Omega} + \|\operatorname{div}(\boldsymbol{\tau})\|_{l,4/3;\Omega} \right\}. \quad (4.29)$$

(\mathbf{AP}_h^{φ}) there exists $C > 0$, independent of h , such that for each $l \in [0, k+1]$, and for each $\psi \in \mathbf{W}^{l,4}(\Omega)$ there holds

$$\operatorname{dist}(\psi, \mathbf{H}_h^{\varphi}) := \inf_{\psi_h \in \mathbf{H}_h^{\varphi}} \|\psi - \psi_h\|_{0,4;\Omega} \leq Ch^l \|\psi\|_{l,4;\Omega}. \quad (4.30)$$

($\mathbf{AP}_h^{\tilde{\mathbf{t}}}$) there exists $C > 0$, independent of h , such that for each $l \in [0, k+1]$, and for each $\tilde{\mathbf{s}} \in \mathbf{H}^l(\Omega)$ there holds

$$\operatorname{dist}(\tilde{\mathbf{s}}, \mathbf{H}_h^{\tilde{\mathbf{t}}}) := \inf_{\tilde{\mathbf{s}}_h \in \mathbf{H}_h^{\tilde{\mathbf{t}}}} \|\tilde{\mathbf{s}} - \tilde{\mathbf{s}}_h\|_{0,\Omega} \leq Ch^l \|\tilde{\mathbf{s}}\|_{l,\Omega}. \quad (4.31)$$

($\mathbf{AP}_h^{\tilde{\sigma}}$) there exists $C > 0$, independent of h , such that for each $l \in [0, k+1]$, and for each $\tilde{\boldsymbol{\tau}} \in \mathbf{H}^l(\Omega) \cap \mathbf{H}(\operatorname{div}_{4/3}; \Omega)$ with $\operatorname{div}(\tilde{\boldsymbol{\tau}}) \in \mathbf{W}^{l,4/3}(\Omega)$, there holds

$$\operatorname{dist}(\tilde{\boldsymbol{\tau}}, \mathbf{H}_h^{\tilde{\sigma}}) := \inf_{\tilde{\boldsymbol{\tau}}_h \in \mathbf{H}_h^{\tilde{\sigma}}} \|\tilde{\boldsymbol{\tau}} - \tilde{\boldsymbol{\tau}}_h\|_{\operatorname{div}_{4/3};\Omega} \leq Ch^l \left\{ \|\tilde{\boldsymbol{\tau}}\|_{l,\Omega} + \|\operatorname{div}(\tilde{\boldsymbol{\tau}})\|_{l,4/3;\Omega} \right\}. \quad (4.32)$$

5. A priori error analysis

The first objective here is to derive a Céa estimate. Let $(\vec{\mathbf{u}}, \boldsymbol{\sigma}) \in \mathbf{H} \times \mathbb{H}_0(\operatorname{div}_{4/3}; \Omega)$ and $(\vec{\boldsymbol{\varphi}}_j, \vec{\boldsymbol{\sigma}}_j) := ((\varphi_j, \tilde{\mathbf{t}}_j), \tilde{\boldsymbol{\sigma}}_j) \in \tilde{\mathbf{H}} \times \mathbf{H}(\operatorname{div}_{4/3}; \Omega)$, $j \in \{1, 2\}$, with $(\mathbf{u}, \boldsymbol{\varphi}) := (\mathbf{u}, (\varphi_1, \varphi_2)) \in W$, be the unique solution of the coupled problem (3.6), and let $(\vec{\mathbf{u}}_h, \boldsymbol{\sigma}_h) \in \mathbf{H}_h \times \mathbb{H}_h^{\sigma}$ and $(\vec{\boldsymbol{\varphi}}_{j,h}, \vec{\boldsymbol{\sigma}}_{j,h}) := ((\varphi_{j,h}, \tilde{\mathbf{t}}_{j,h}), \tilde{\boldsymbol{\sigma}}_{j,h}) \in \tilde{\mathbf{H}}_h \times \mathbf{H}_h^{\tilde{\sigma}}$,

with $(\mathbf{u}_h, \boldsymbol{\varphi}_h) := (\mathbf{u}_h, (\varphi_{1,h}, \varphi_{2,h})) \in W_h$, be a solution of the discrete coupled problem (4.1). Then, we first rewrite (3.6) and (4.1) in terms of the forms (3.26) and (3.27), that is

$$\begin{aligned} \mathcal{A}_{\mathbf{u}, \boldsymbol{\varphi}}(\vec{\mathbf{u}}, \vec{\mathbf{v}}) + b(\vec{\mathbf{v}}, \boldsymbol{\sigma}) &= F_{\boldsymbol{\varphi}}(\vec{\mathbf{v}}) & \forall \vec{\mathbf{v}} \in \mathbf{H}, \\ b(\vec{\mathbf{u}}, \boldsymbol{\tau}) &= G(\boldsymbol{\tau}) & \forall \boldsymbol{\tau} \in \mathbb{H}_0(\operatorname{div}_{4/3}; \Omega), \end{aligned} \quad (5.1)$$

$$\begin{aligned} \tilde{\mathcal{A}}_{\mathbf{u}, j}(\vec{\boldsymbol{\varphi}}_j, \vec{\boldsymbol{\psi}}_j) + \tilde{b}(\vec{\boldsymbol{\psi}}_j, \tilde{\boldsymbol{\sigma}}_j) &= 0 & \forall \vec{\boldsymbol{\psi}}_j \in \tilde{\mathbf{H}}, \\ \tilde{b}(\vec{\boldsymbol{\varphi}}_j, \tilde{\boldsymbol{\tau}}_j) &= \tilde{G}_j(\tilde{\boldsymbol{\tau}}_j) & \forall \tilde{\boldsymbol{\tau}}_j \in \mathbf{H}(\operatorname{div}_{4/3}; \Omega), \end{aligned} \quad (5.2)$$

$$\begin{aligned} \mathcal{A}_{\mathbf{u}_h, \boldsymbol{\varphi}_h}(\vec{\mathbf{u}}_h, \vec{\mathbf{v}}_h) + b(\vec{\mathbf{v}}_h, \boldsymbol{\sigma}_h) &= F_{\boldsymbol{\varphi}_h}(\vec{\mathbf{v}}_h) & \forall \vec{\mathbf{v}}_h \in \mathbf{H}_h, \\ b(\vec{\mathbf{u}}_h, \boldsymbol{\tau}_h) &= G(\boldsymbol{\tau}_h) & \forall \boldsymbol{\tau}_h \in \mathbb{H}_h^{\boldsymbol{\sigma}}, \end{aligned} \quad (5.3)$$

and

$$\begin{aligned} \tilde{\mathcal{A}}_{\mathbf{u}_h, j}(\vec{\boldsymbol{\varphi}}_{j,h}, \vec{\boldsymbol{\psi}}_{j,h}) + \tilde{b}(\vec{\boldsymbol{\psi}}_{j,h}, \tilde{\boldsymbol{\sigma}}_{j,h}) &= 0 & \forall \vec{\boldsymbol{\psi}}_{j,h} \in \tilde{\mathbf{H}}_h, \\ \tilde{b}(\vec{\boldsymbol{\varphi}}_{j,h}, \tilde{\boldsymbol{\tau}}_{j,h}) &= \tilde{G}_j(\tilde{\boldsymbol{\tau}}_{j,h}) & \forall \tilde{\boldsymbol{\tau}}_{j,h} \in \mathbf{H}_h^{\tilde{\boldsymbol{\sigma}}}. \end{aligned} \quad (5.4)$$

Applying the Strang lemma stated in [22, Lemma 6.1] to the context given by problems (5.1) and (5.3) (resp. problems (5.2) and (5.4)), and bearing in mind similar consistency estimates to those provided in [22, eqs. (6.16) and (6.18)] (resp. [22, eq. (6.17)]), we find, respectively, that

$$\begin{aligned} \|(\vec{\mathbf{u}}, \boldsymbol{\sigma}) - (\vec{\mathbf{u}}_h, \boldsymbol{\sigma}_h)\| &\leq \bar{C}_{S,1} \operatorname{dist}(\vec{\mathbf{u}}, \mathbf{H}_h) + \bar{C}_{S,2} \operatorname{dist}(\boldsymbol{\sigma}, \mathbb{H}_h^{\boldsymbol{\sigma}}) \\ &\quad + \bar{C}_{S,3} c(\mathbf{g}, \mathbf{u}_D) \left\{ \|\varphi_1 - \varphi_{1,h}\|_{0,4;\Omega} + \|\varphi_2 - \varphi_{2,h}\|_{0,4;\Omega} + \|\mathbf{u} - \mathbf{u}_h\|_{0,4;\Omega} \right\}, \end{aligned} \quad (5.5)$$

and for each $j \in \{1, 2\}$, the bound

$$\|(\vec{\boldsymbol{\varphi}}_j, \tilde{\boldsymbol{\sigma}}_j) - (\vec{\boldsymbol{\varphi}}_{j,h}, \tilde{\boldsymbol{\sigma}}_{j,h})\| \leq \hat{C}_{S,1} \operatorname{dist}(\vec{\boldsymbol{\varphi}}_j, \tilde{\mathbf{H}}_h) + \hat{C}_{S,2} \operatorname{dist}(\tilde{\boldsymbol{\sigma}}_j, \mathbf{H}_h^{\tilde{\boldsymbol{\sigma}}}) + \hat{C}_{S,3} c(\boldsymbol{\varphi}_D) \|\mathbf{u} - \mathbf{u}_h\|_{0,4;\Omega}. \quad (5.6)$$

For the remaining expressions in (5.5)-(5.6), note that $c(\mathbf{g}, \mathbf{u}_D)$ depends linearly on $\|\mathbf{g}\|_{0,\infty;\Omega}$ and $\|\mathbf{u}_D\|_{1/2,\Gamma}$, whereas $\bar{C}_{S,1}$, $\bar{C}_{S,2}$, and $\bar{C}_{S,3}$ are positive constants computed using [22, eq. (6.4)] and depending on $\mu_2, \boldsymbol{\nu}, r, \alpha_a, \beta_a$. After using (3.28), these constants are used to bound both $\|\mathcal{A}_{\mathbf{u}, \boldsymbol{\varphi}}\|$ and $\|\mathcal{A}_{\mathbf{u}_h, \boldsymbol{\varphi}_h}\|$ by $(|\Omega|^{1/2} \gamma + 2\mu_2 + r)$. In turn, $c(\boldsymbol{\varphi}_D)$ is a constant multiple of $\|\boldsymbol{\varphi}_D\|_{1/2,\Gamma}$, and $\hat{C}_{S,1}$, $\hat{C}_{S,2}$. Also, $\hat{C}_{S,3}$ are positive constants defined in terms of $\|\mathbb{K}\|_{0,\infty;\Omega}$, r , $\tilde{\alpha}_a$, and $\tilde{\beta}_a$, which are computed according to [22, eq. (6.4)], after using (3.29) to bound both $\|\tilde{\mathcal{A}}_{\mathbf{u}, j}\|$ and $\|\tilde{\mathcal{A}}_{\mathbf{u}_h, j}\|$ by $(\|\mathbb{K}\|_{0,\infty;\Omega} + r)$.

Next we can insert (5.6) into (5.5), which leads to

$$\begin{aligned} \|(\vec{\mathbf{u}}, \boldsymbol{\sigma}) - (\vec{\mathbf{u}}_h, \boldsymbol{\sigma}_h)\| &\leq \bar{C}_{S,1} \operatorname{dist}(\vec{\mathbf{u}}, \mathbf{H}_h) + \bar{C}_{S,2} \operatorname{dist}(\boldsymbol{\sigma}, \mathbb{H}_h^{\boldsymbol{\sigma}}) \\ &\quad + \bar{C}_{S,3} c(\mathbf{g}, \mathbf{u}_D) \hat{C}_{S,1} \sum_{j=1}^2 \operatorname{dist}(\vec{\boldsymbol{\varphi}}_j, \tilde{\mathbf{H}}_h) \\ &\quad + \bar{C}_{S,3} c(\mathbf{g}, \mathbf{u}_D) \hat{C}_{S,2} \sum_{j=1}^2 \operatorname{dist}(\tilde{\boldsymbol{\sigma}}_j, \mathbf{H}_h^{\tilde{\boldsymbol{\sigma}}}) \\ &\quad + \bar{C}_{S,3} c(\mathbf{g}, \mathbf{u}_D) \{1 + 2\hat{C}_{S,3} c(\boldsymbol{\varphi}_D)\} \|\mathbf{u} - \mathbf{u}_h\|_{0,4;\Omega}. \end{aligned} \quad (5.7)$$

Imposing the constant multiplying $\|\mathbf{u} - \mathbf{u}_h\|_{0,4;\Omega}$ in (5.7) to be sufficiently small, say $\leq 1/2$, we derive the a priori upper bound for $\|(\vec{\mathbf{u}}, \boldsymbol{\sigma}) - (\vec{\mathbf{u}}_h, \boldsymbol{\sigma}_h)\|$. Hence, employing this latter estimate to bound the third term on the right-hand side of (5.6), we deduce the corresponding upper bound for $\|(\vec{\boldsymbol{\varphi}}_j, \tilde{\boldsymbol{\sigma}}_j) - (\vec{\boldsymbol{\varphi}}_{j,h}, \tilde{\boldsymbol{\sigma}}_{j,h})\|$, $j \in \{1, 2\}$. We have thus demonstrated the following result.

Theorem 5.1. *Assume that the data \mathbf{g} , \mathbf{u}_D , and φ_D satisfy*

$$\bar{C}_{S,3}c(\mathbf{g}, \mathbf{u}_D)\{1 + 2\widehat{C}_{S,3}c(\varphi_D)\} \leq \frac{1}{2}.$$

Then, there exists a positive constant C , independent of h , but depending on μ_2 , $\boldsymbol{\vartheta}$, r , α_a , β_a , $\|\mathbb{K}\|_{0,\infty;\Omega}$, $\tilde{\alpha}_a$, $\tilde{\beta}_a$, $\|\mathbf{g}\|_{0,\infty;\Omega}$, $\|\mathbf{u}_D\|_{1/2,\Gamma}$, and $\|\varphi_D\|_{1/2,\Gamma}$, such that

$$\begin{aligned} & \|(\vec{\mathbf{u}}, \boldsymbol{\sigma}) - (\vec{\mathbf{u}}_h, \boldsymbol{\sigma}_h)\| + \sum_{j=1}^2 \|(\vec{\boldsymbol{\varphi}}_j, \tilde{\boldsymbol{\sigma}}_j) - (\vec{\boldsymbol{\varphi}}_{j,h}, \tilde{\boldsymbol{\sigma}}_{j,h})\| \\ & \leq C \left\{ \text{dist}(\vec{\mathbf{u}}, \mathbf{H}_h) + \text{dist}(\boldsymbol{\sigma}, \mathbb{H}_h^\sigma) + \sum_{j=1}^2 \left(\text{dist}(\vec{\boldsymbol{\varphi}}_j, \tilde{\mathbf{H}}_h) + \text{dist}(\tilde{\boldsymbol{\sigma}}_j, \mathbf{H}_h^{\tilde{\boldsymbol{\sigma}}}) \right) \right\}. \end{aligned} \quad (5.8)$$

We are now able to provide the rates of convergence of the Galerkin scheme (4.1) when the finite element subspaces specified in Section 4.3 are employed.

Theorem 5.2. *Assume that there exists $l \in [0, k + 1]$ such that $\mathbf{u} \in \mathbf{W}^{l,4}(\Omega)$, $\mathbf{t} \in \mathbb{H}^l(\Omega) \cap \mathbb{L}_{\text{tr}}^2(\Omega)$, $\boldsymbol{\sigma} \in \mathbb{H}^l(\Omega) \cap \mathbb{H}_0(\mathbf{div}_{4/3}; \Omega)$, $\mathbf{div}(\boldsymbol{\sigma}) \in \mathbf{W}^{l,4/3}(\Omega)$, $\varphi_j \in \mathbf{W}^{l,4}(\Omega)$, $\tilde{\mathbf{t}}_j \in \mathbf{H}^l(\Omega)$, $\tilde{\boldsymbol{\sigma}}_j \in \mathbf{H}^l(\Omega) \cap \mathbf{H}(\mathbf{div}_{4/3}; \Omega)$, and $\mathbf{div}(\tilde{\boldsymbol{\sigma}}_j) \in \mathbf{W}^{l,4/3}(\Omega)$, for $j \in \{1, 2\}$. Then, there exists $C > 0$, independent of h , such that*

$$\begin{aligned} & \|(\vec{\mathbf{u}}, \boldsymbol{\sigma}) - (\vec{\mathbf{u}}_h, \boldsymbol{\sigma}_h)\| + \sum_{j=1}^2 \|(\vec{\boldsymbol{\varphi}}_j, \tilde{\boldsymbol{\sigma}}_j) - (\vec{\boldsymbol{\varphi}}_{j,h}, \tilde{\boldsymbol{\sigma}}_{j,h})\| \\ & \leq Ch^l \left\{ \|\mathbf{u}\|_{l,4;\Omega} + \|\mathbf{t}\|_{l,\Omega} + \|\boldsymbol{\sigma}\|_{l,\Omega} \right. \\ & \quad \left. + \|\mathbf{div}(\boldsymbol{\sigma})\|_{l,4/3;\Omega} + \sum_{j=1}^2 \left\{ \|\varphi_j\|_{l,4;\Omega} + \|\tilde{\mathbf{t}}_j\|_{l,\Omega} + \|\tilde{\boldsymbol{\sigma}}_j\|_{l,\Omega} + \|\mathbf{div}(\tilde{\boldsymbol{\sigma}}_j)\|_{l,4/3;\Omega} \right\} \right\}. \end{aligned} \quad (5.9)$$

Proof. It follows straightforwardly from (5.8) and the approximation properties from Section 4.3. ■

We end this section with the derivative-free postprocessing of the pressure. From the orthogonal decomposition for the pseudostress tensor (3.3) (which yielded the new tensor unknown $\boldsymbol{\sigma} \in \mathbb{H}_0(\mathbf{div}_{4/3}; \Omega)$), we deduce that (2.5) becomes

$$p = -\frac{1}{2n} \text{tr}(2\boldsymbol{\sigma} + 2c\mathbb{I} + \mathbf{u} \otimes \mathbf{u}), \quad \text{with} \quad c := -\frac{1}{2n|\Omega|} \int_{\Omega} \text{tr}(\mathbf{u} \otimes \mathbf{u}).$$

And therefore the discrete pressure will be defined as

$$p_h := -\frac{1}{2n} \text{tr}(2\boldsymbol{\sigma}_h + 2c_h\mathbb{I} + \mathbf{u}_h \otimes \mathbf{u}_h), \quad \text{with} \quad c_h := -\frac{1}{2n|\Omega|} \int_{\Omega} \text{tr}(\mathbf{u}_h \otimes \mathbf{u}_h).$$

Moreover, it is easy to prove that there exists a positive constant C , independent of h , such that

$$\|p - p_h\|_{0,\Omega} \leq C \left\{ \|\boldsymbol{\sigma} - \boldsymbol{\sigma}_h\|_{\mathbf{div}_{4/3};\Omega} + \|\mathbf{u} - \mathbf{u}_h\|_{0,4;\Omega} \right\},$$

whence the rate of convergence of p_h coincides with the one established by (5.9).

6. A posteriori error estimator

In this section we propose a reliable and efficient residual-based a posteriori error estimator for the Galerkin scheme (4.1) in both the 2D and 3D cases. To this end, we first recall from Section 4.3 that, given a regular partition \mathcal{T}_h of Ω into triangles (in \mathbb{R}^2) or tetrahedra (in \mathbb{R}^3), its barycentric refinement is denoted by \mathcal{T}_h^b .

6.1. The 2D case

We let \mathcal{E}_h be the set of all edges of \mathcal{T}_h^b , and denote by $\mathcal{E}_h(K)$ the set of edges of a given $K \in \mathcal{T}_h^b$. Then, we split $\mathcal{E}_h = \mathcal{E}_h(\Omega) \cup \mathcal{E}_h(\Gamma)$, where $\mathcal{E}_h(\Omega) := \{e \in \mathcal{E}_h : e \in \Omega\}$ and $\mathcal{E}_h(\Gamma) := \{e \in \mathcal{E}_h : e \in \Gamma\}$. In turn, h_e stands for the length of a given edge e , and for each edge $e \in \mathcal{E}_h$ we fix a unit normal vector $\boldsymbol{\nu}_e := (\nu_1, \nu_2)^\top$, and let $\mathbf{s}_e := (-\nu_2, \nu_1)^\top$ be the corresponding fixed unit tangential vector along e . However, when no confusion arises, we simply write $\boldsymbol{\nu}$ and \mathbf{s} instead of $\boldsymbol{\nu}_e$ and \mathbf{s}_e , respectively. Now, let $\mathbf{v} \in \mathbf{L}^2(\Omega)$ such that $\mathbf{v}|_K \in \mathbf{C}(K)$ on each $K \in \mathcal{T}_h^b$. Then, given $K \in \mathcal{T}_h^b$ and $e \in \mathcal{E}(K) \cap \mathcal{E}_h(\Omega)$, we denote by $\llbracket \mathbf{v} \cdot \mathbf{s} \rrbracket$ the tangential jump of \mathbf{v} across e , that is, $\llbracket \mathbf{v} \cdot \mathbf{s} \rrbracket := (\mathbf{v}|_K - \mathbf{v}|_{K'})|_e \cdot \mathbf{s}$, where K and K' are the triangles of \mathcal{T}_h^b having e as a common edge. A similar definition holds for the tangential jump of a tensor field $\boldsymbol{\tau} \in \mathbf{L}^2(\Omega)$ such that $\boldsymbol{\tau}|_K \in \mathbf{C}(K)$. Finally, given sufficiently smooth scalar, vector and matrix valued fields ϕ , $\mathbf{v} = (v_1, v_2)^\top$ and $\boldsymbol{\tau} := (\tau_{ij})_{2 \times 2}$, respectively, we set

$$\begin{aligned} \mathbf{curl}(\phi) &:= \left(\frac{\partial \phi}{\partial x_2}, -\frac{\partial \phi}{\partial x_1} \right)^\top, & \underline{\mathbf{curl}}(\mathbf{v}) &:= \begin{pmatrix} \mathbf{curl}(v_1) \\ \mathbf{curl}(v_2) \end{pmatrix}, \\ \mathbf{rot}(\mathbf{v}) &:= \frac{\partial v_2}{\partial x_1} - \frac{\partial v_1}{\partial x_2}, & \mathbf{rot}(\boldsymbol{\tau}) &:= \begin{pmatrix} \mathbf{rot}(\tau_{11}, \tau_{12}) \\ \mathbf{rot}(\tau_{21}, \tau_{22}) \end{pmatrix}. \end{aligned}$$

Then, recalling that the solution of the discrete coupled problem (4.1) is given by $(\vec{\mathbf{u}}_h, \boldsymbol{\sigma}_h) \in \mathbf{H}_h \times \mathbb{H}_h^\sigma$ and $(\vec{\boldsymbol{\varphi}}_{j,h}, \vec{\boldsymbol{\sigma}}_{j,h}) := ((\varphi_{j,h}, \tilde{\mathbf{t}}_{j,h}), \tilde{\boldsymbol{\sigma}}_{j,h}) \in \tilde{\mathbf{H}}_h \times \mathbf{H}_h^{\tilde{\boldsymbol{\sigma}}}$, with $(\mathbf{u}_h, \boldsymbol{\varphi}_h) := (\mathbf{u}_h, (\varphi_{1,h}, \varphi_{2,h})) \in W_h$, and assuming that the data \mathbf{u}_D and $\boldsymbol{\varphi}_D$ belong to $\mathbf{H}^1(\Gamma)$, we introduce for each $K \in \mathcal{T}_h^b$ the local a posteriori error indicators:

$$\tilde{\Psi}_K^{4/3} := \|\gamma \mathbf{u}_h - \mathbf{div} \boldsymbol{\sigma}_h + \frac{1}{2} \mathbf{t}_h \mathbf{u}_h - (\boldsymbol{\vartheta} \cdot \boldsymbol{\varphi}_h) \mathbf{g}\|_{0,4/3;K}^{4/3} + \sum_{j=1}^2 \|\mathbf{div} \tilde{\boldsymbol{\sigma}}_{j,h} - \frac{1}{2} \mathbf{u}_h \cdot \tilde{\mathbf{t}}_{j,h}\|_{0,4/3;K}^{4/3}, \quad (6.1)$$

$$\begin{aligned} \hat{\Psi}_K^2 &:= \|2\mu(\boldsymbol{\varphi}_h) \mathbf{t}_{h,sym} - \frac{1}{2} (\mathbf{u}_h \otimes \mathbf{u}_h)^d - \boldsymbol{\sigma}_h^d\|_{0,K}^2 + h_K^2 \|\mathbf{rot}(\mathbf{t}_h)\|_{0,K}^2 \\ &+ \sum_{e \in \mathcal{E}_h(K) \cap \mathcal{E}_h(\Omega)} h_e \|\llbracket \mathbf{t}_h \mathbf{s} \rrbracket\|_{0,e}^2 + \sum_{e \in \mathcal{E}_h(K) \cap \mathcal{E}_h(\Gamma)} h_e \|\mathbf{t}_h \mathbf{s} - \nabla \mathbf{u}_D \mathbf{s}\|_{0,e}^2 \\ &+ \sum_{j=1}^2 \left\{ \|\mathbb{K}_j \tilde{\mathbf{t}}_{j,h} - \frac{1}{2} \varphi_{j,h} \mathbf{u}_h - \tilde{\boldsymbol{\sigma}}_{j,h}\|_{0,K}^2 + h_K^2 \|\mathbf{rot}(\tilde{\mathbf{t}}_{j,h})\|_{0,K}^2 \right. \\ &\quad \left. + \sum_{e \in \mathcal{E}_h(K) \cap \mathcal{E}_h(\Omega)} h_e \|\llbracket \tilde{\mathbf{t}}_{j,h} \cdot \mathbf{s} \rrbracket\|_{0,e}^2 + \sum_{e \in \mathcal{E}_h(K) \cap \mathcal{E}_h(\Gamma)} h_e \|\tilde{\mathbf{t}}_{j,h} \cdot \mathbf{s} - \nabla \varphi_{j,D} \cdot \mathbf{s}\|_{0,e}^2 \right\}, \end{aligned} \quad (6.2)$$

and

$$\begin{aligned} \bar{\Psi}_K^4 &:= h_K^4 \|\mathbf{t}_h - \nabla \mathbf{u}_h\|_{0,4;K}^4 + \sum_{e \in \mathcal{E}_h(K) \cap \mathcal{E}_h(\Gamma)} h_e^2 \|\mathbf{u}_D - \mathbf{u}_h\|_{0,e}^4 \\ &+ \sum_{j=1}^2 \left\{ h_K^4 \|\tilde{\mathbf{t}}_{j,h} - \nabla \varphi_{j,h}\|_{0,4;K}^4 + \sum_{e \in \mathcal{E}_h(K) \cap \mathcal{E}_h(\Gamma)} h_e^2 \|\varphi_{j,D} - \varphi_{j,h}\|_{0,e}^4 \right\}. \end{aligned} \quad (6.3)$$

It is important to stress here the residual character of each one of the terms defining the foregoing indicators, which follows from the equations defining the strong coupled problem (2.8) and the regularity of the solution of the continuous formulation (3.6).

Next, we define the global, and fully computable, a posteriori error estimator as

$$\Psi = \left\{ \sum_{K \in \mathcal{T}_h^b} \tilde{\Psi}_K^{4/3} \right\}^{3/4} + \left\{ \sum_{K \in \mathcal{T}_h^b} \hat{\Psi}_K^2 \right\}^{1/2} + \left\{ \sum_{K \in \mathcal{T}_h^b} \bar{\Psi}_K^4 \right\}^{1/4}. \quad (6.4)$$

In this way, recalling now that the solution of the continuous coupled problem (3.6) is given by $(\vec{\mathbf{u}}, \boldsymbol{\sigma}) \in \mathbf{H} \times \mathbb{H}_0(\mathbf{div}_{4/3}; \Omega)$ and $(\vec{\boldsymbol{\varphi}}_j, \tilde{\boldsymbol{\sigma}}_j) := ((\varphi_j, \tilde{\mathbf{t}}_j), \tilde{\boldsymbol{\sigma}}_j) \in \tilde{\mathbf{H}} \times \mathbf{H}(\mathbf{div}_{4/3}; \Omega)$, $j \in \{1, 2\}$, with $(\mathbf{u}, \boldsymbol{\varphi}) := (\mathbf{u}, (\varphi_1, \varphi_2)) \in W$, we are able to establish the following main result.

Theorem 6.1. *Assume for simplicity that \mathbf{u}_D and φ_D are piecewise polynomials. Then there exist positive constants C_{rel} and C_{eff} , independent of h , such that*

$$C_{\text{eff}} \Psi + \text{h.o.t.} \leq \|(\vec{\mathbf{u}}, \boldsymbol{\sigma}) - (\vec{\mathbf{u}}_h, \boldsymbol{\sigma}_h)\| + \sum_{j=1}^2 \|(\vec{\boldsymbol{\varphi}}_j, \tilde{\boldsymbol{\sigma}}_j) - (\vec{\boldsymbol{\varphi}}_{j,h}, \tilde{\boldsymbol{\sigma}}_{j,h})\| \leq C_{\text{rel}} \Psi, \quad (6.5)$$

where *h.o.t.* stands for one or several terms of higher order, including the oscillation of the forcing terms and the Dirichlet data.

The proof of Theorem 6.1 will be reported with full details in the forthcoming work [31]. For the moment we mention that the upper bound in (6.5) (known as the reliability estimate), is derived using global inf-sup conditions, suitable Helmholtz decompositions in Banach spaces, the approximation properties of the Raviart–Thomas and Clément interpolants, and regularity and smallness assumptions on the data. On the other hand, the lower bound in (6.5) (efficiency), is proved by means of inverse inequalities and localization techniques based on bubble functions.

6.2. The 3D case

Given a tetrahedron $K \in \mathcal{T}_h^b$, we now let $\mathcal{E}(K)$ be the set of its faces, and let \mathcal{E}_h be the set of all faces of the triangulation \mathcal{T}_h^d with the corresponding analogue decomposition $\mathcal{E}_h = \mathcal{E}_h(\Omega) \cup \mathcal{E}_h(\Gamma)$. Then, for each face $e \in \mathcal{E}_h$ we fix a unit normal $\boldsymbol{\nu}_e$ to e . As before, when no confusion arises, we simply write $\boldsymbol{\nu}$ instead of $\boldsymbol{\nu}_e$. In this way, given $\mathbf{v} \in \mathbf{L}^2(\Omega)$ such that $\mathbf{v}|_K \in \mathbf{C}(K)$ for each $K \in \mathcal{T}_h^b$, and $e \in \mathcal{E}(K) \cap \mathcal{E}_h(\Omega)$, we denote by $\llbracket \mathbf{v} \times \boldsymbol{\nu} \rrbracket$ the tangential jump of \mathbf{v} across e , that is, $\llbracket \mathbf{v} \times \boldsymbol{\nu} \rrbracket := (\mathbf{v}|_K - \mathbf{v}|_{K'})|_e \times \boldsymbol{\nu}$, where K and K' are the tetrahedron of \mathcal{T}_h^b having e as a common face. Similarly, given $\boldsymbol{\tau} \in \mathbb{L}^2(\Omega)$ such that $\boldsymbol{\tau}|_K \in \mathbf{C}(K)$, we let $\llbracket \boldsymbol{\tau} \times \boldsymbol{\nu} \rrbracket$ be the tangential jump of $\boldsymbol{\tau}$ across e , that is $\llbracket \boldsymbol{\tau} \times \boldsymbol{\nu} \rrbracket := (\boldsymbol{\tau}|_K - \boldsymbol{\tau}|_{K'})|_e \times \boldsymbol{\nu}$. Next, we recall that the curl of a 3-D vector $\mathbf{v} := (v_1, v_2, v_3)$ is the 3-D vector

$$\mathbf{curl}(\mathbf{v}) = \nabla \times \mathbf{v} := \left(\frac{\partial v_3}{\partial x_2} - \frac{\partial v_2}{\partial x_3}, \frac{\partial v_1}{\partial x_3} - \frac{\partial v_3}{\partial x_1}, \frac{\partial v_2}{\partial x_1} - \frac{\partial v_1}{\partial x_2} \right),$$

and that, given a tensor function $\boldsymbol{\tau} := (\tau_{ij})_{3 \times 3}$, the operator $\mathbf{curl}(\boldsymbol{\tau})$ is the 3×3 tensor whose rows are given by

$$\mathbf{curl}(\boldsymbol{\tau}) := \begin{pmatrix} \mathbf{curl}(\tau_{11}, \tau_{12}, \tau_{13}) \\ \mathbf{curl}(\tau_{21}, \tau_{22}, \tau_{23}) \\ \mathbf{curl}(\tau_{31}, \tau_{32}, \tau_{33}) \end{pmatrix}.$$

In turn, $\boldsymbol{\tau} \times \boldsymbol{\nu}$ stands for the 3×3 tensor whose rows are given by the tangential components of each row of $\boldsymbol{\tau}$. In addition, the tangential curl operator \mathbf{curl}_s and a tensor version of it, denoted \mathbf{curl}_s , which is defined component-wise by \mathbf{curl}_s , will also be utilized (see. e.g. [18, Section 3] for details).

Then, the local a posteriori error indicators and the global a posteriori error estimator Ψ are defined in this case exactly as in the previous section, except that $\widehat{\Psi}_K^2$ (cf. (6.2)) is replaced for each $K \in \mathcal{T}_h^{\mathfrak{b}}$ by the following slightly modified expression

$$\begin{aligned}
 \widehat{\Psi}_K^2 &:= \left\| 2\mu(\varphi_h)\mathbf{t}_{h,sym} - \frac{1}{2}(\mathbf{u}_h \otimes \mathbf{u}_h)^{\mathfrak{d}} - \boldsymbol{\sigma}_h^{\mathfrak{d}} \right\|_{0,K}^2 + h_K^2 \|\mathbf{curl}(\mathbf{t}_h)\|_{0,K}^2 \\
 &+ \sum_{e \in \mathcal{E}_h(K) \cap \mathcal{E}_h(\Omega)} h_e \|\llbracket \mathbf{t}_h \times \boldsymbol{\nu} \rrbracket\|_{0,e}^2 + \sum_{e \in \mathcal{E}_h(K) \cap \mathcal{E}_h(\Gamma)} h_e \|\mathbf{t}_h \times \boldsymbol{\nu} - \mathbf{curl}_s \mathbf{u}_D\|_{0,e}^2 \\
 &+ \sum_{j=1}^2 \left\{ \|\mathbb{K}_j \tilde{\mathbf{t}}_{j,h} - \frac{1}{2} \varphi_{j,h} \mathbf{u}_h - \tilde{\boldsymbol{\sigma}}_{j,h}\|_{0,K}^2 + h_K^2 \|\mathbf{curl}(\tilde{\mathbf{t}}_{j,h})\|_{0,K}^2 \right. \\
 &\quad \left. + \sum_{e \in \mathcal{E}_h(K) \cap \mathcal{E}_h(\Omega)} h_e \|\llbracket \tilde{\mathbf{t}}_{j,h} \times \boldsymbol{\nu} \rrbracket\|_{0,e}^2 + \sum_{e \in \mathcal{E}_h(K) \cap \mathcal{E}_h(\Gamma)} h_e \|\tilde{\mathbf{t}}_{j,h} \times \boldsymbol{\nu} - \mathbf{curl}_s \varphi_{j,D}\|_{0,e}^2 \right\}.
 \end{aligned} \tag{6.6}$$

Similarly as we observed in the previous section for all the local a posteriori error indicators, it is easy to realize that the terms defining the 3D version of $\widehat{\Psi}_K^2$ (cf. (6.6)) are of residual character as well.

Finally, the analogue of Theorem 6.1 also holds in this 3D case, and the same remark given at the end of Section 6.1 is valid here for its respective proof.

6.3. The adaptive refinement algorithm

We now turn to define, according to the above local a posteriori error indicators, the following adaptive refinement algorithm based on the classical procedures of solving \rightarrow estimating \rightarrow marking \rightarrow refining, provided in, e.g., [47]. Note that we need to deal with the adaptive procedure associated with the initial triangular/tetrahedral mesh at each refinement step, and still perform an additional step to treat its Alfled split.

- (1) Start with a coarse mesh \mathcal{T}_h made of triangles (or tetrahedra) Δ ,
- (2) Generate the associated barycentric refinement $\mathcal{T}_h^{\mathfrak{b}}$ made of triangles (or tetrahedra) K ,
- (3) Solve the discrete problem (4.1) for the current mesh $\mathcal{T}_h^{\mathfrak{b}}$,
- (4) For each $K \in \mathcal{T}_h^{\mathfrak{b}}$ compute $\tilde{\Psi}_K$, $\widehat{\Psi}_K$, and $\bar{\Psi}_K$, and then $\Psi_K := \tilde{\Psi}_K + \widehat{\Psi}_K + \bar{\Psi}_K$,
- (5) For each $\Delta \in \mathcal{T}_h$ compute the local a posteriori error indicator $\Psi_\Delta := \sum_{K \in \mathcal{T}_h^{\mathfrak{b}}, K \subseteq \Delta} \Psi_K$,
- (6) Check the stopping criteria on \mathcal{T}_h (marking sufficiently many elements so that they represent a given fraction of the total estimated error) and decide whether to finish or continue to the next step,
- (7) Generate an adapted mesh from \mathcal{T}_h through a variable metric/Delaunay automatic meshing algorithm using the local indicators Ψ_Δ , targeting the equidistribution of the local error indicators in the updated mesh (see e.g. [26]),
- (8) Define the resulting mesh as \mathcal{T}_h and go to step (2).

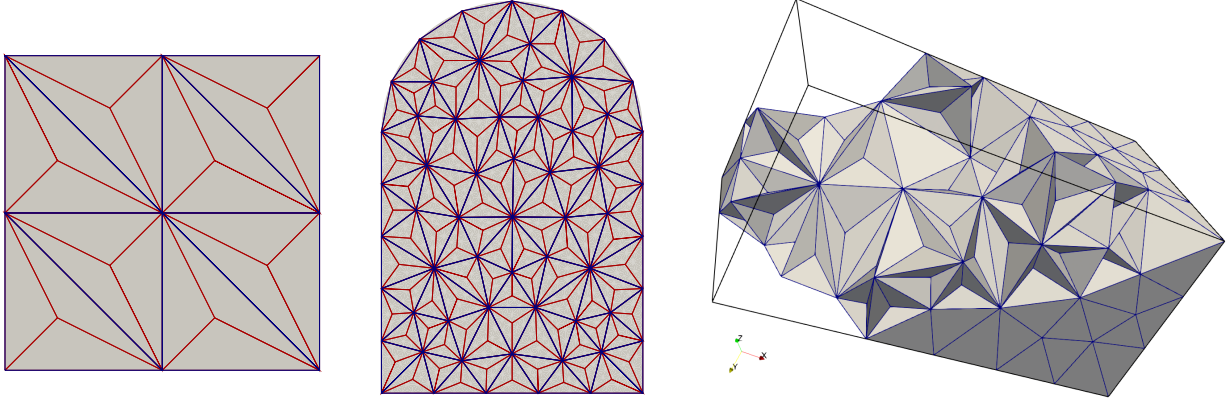


FIGURE 7.1. Example of Alfeld splits for a coarse 2D uniform mesh used in Example 1 (left), a coarse unstructured grid for Example 2 (center), and for a 3D non-uniform mesh used in Example 3 (crinkle clip on the right panel).

7. Numerical results

In this section we present several computational examples confirming the good performance of the fully-mixed finite element method (4.1) with the subspaces indicated in Section 4.3. As required for the stability of the Scott-Vogelius pair, the computations are performed on barycentrically refined meshes \mathcal{T}_h^b created from regular partitions \mathcal{T}_h of Ω , illustrated for 2D and 3D in Figure 7.1. All initial grids and Alfeld splits (barycentric refinements) are generated with the open-source mesh manipulator GMSH [33] and the computational implementation has been carried out using the open-source finite element library FEniCS [8]. A Newton–Raphson algorithm with null initial guesses is used for the resolution of the nonlinear problem (4.1). As usual, the iterative method is finished when the relative error between two consecutive iterations of the complete coefficient vector, namely \mathbf{coeff}^{m+1} and \mathbf{coeff}^m , is sufficiently small, that is,

$$\frac{\|\mathbf{coeff}^{m+1} - \mathbf{coeff}^m\|_{\ell^2}}{\|\mathbf{coeff}^{m+1}\|_{\ell^2}} < \mathbf{tol},$$

where \mathbf{tol} is a specified tolerance and $\|\cdot\|_{\ell^2}$ is the standard ℓ^2 -norm in \mathbb{R}^{DoF} with DoF denoting the total number of degrees of freedom generated by the finite element subspaces. The condition of zero-average pressure (translated in terms of the trace of $2\boldsymbol{\sigma} + \mathbf{u} \otimes \mathbf{u}$) is imposed through a real Lagrange multiplier. The solution of all linear systems is carried out with the multifrontal massively parallel sparse direct solver MUMPS.

Errors between exact and approximate solutions are denoted as

$$\begin{aligned} e(\mathbf{u}) &:= \|\mathbf{u} - \mathbf{u}_h\|_{0,4;\Omega}, & e(\mathbf{t}) &:= \|\mathbf{t} - \mathbf{t}_h\|_{0,\Omega} & e(\boldsymbol{\sigma}) &:= \|\boldsymbol{\sigma} - \boldsymbol{\sigma}_h\|_{\text{div}_{4/3};\Omega}, & e(p) &:= \|p - p_h\|_{0,\Omega}, \\ e(\boldsymbol{\varphi}) &:= \sum_{j=1}^2 \|\varphi_j - \varphi_{j,h}\|_{0,4;\Omega}, & e(\tilde{\mathbf{t}}) &:= \sum_{j=1}^2 \|\tilde{\mathbf{t}}_j - \tilde{\mathbf{t}}_{j,h}\|_{0,4;\Omega}, & e(\tilde{\boldsymbol{\sigma}}) &:= \sum_{j=1}^2 \|\tilde{\boldsymbol{\sigma}}_j - \tilde{\boldsymbol{\sigma}}_{j,h}\|_{\text{div}_{4/3};\Omega}. \end{aligned}$$

In turn, we let $r(\star)$ be their corresponding rates of convergence, that is

$$r(\star) := \frac{\log(e(\star)/e'(\star))}{\log(h/h')} \quad \forall \star \in \{\mathbf{u}, \mathbf{t}, \boldsymbol{\sigma}, p, \boldsymbol{\varphi}, \tilde{\mathbf{t}}, \tilde{\boldsymbol{\sigma}}\},$$

where h and h' denote two consecutive mesh sizes with errors $e(\star)$ and $e'(\star)$, respectively.

Finite Element Family: $\mathbf{P}_1 - \mathbb{P}_1 - \mathbb{RT}_1 - \mathbf{P}_1 - \mathbb{P}_1 - \mathbb{RT}_1$								
DoF	h	$e(\mathbf{u})$	$r(\mathbf{u})$	$e(\mathbf{t})$	$r(\mathbf{t})$	$e(\boldsymbol{\sigma})$	$r(\boldsymbol{\sigma})$	
1305	1.4140	0.0902	–	0.5561	–	0.9379	–	
5153	0.7071	0.0213	2.222	0.1996	1.682	0.2785	1.752	
20481	0.3536	0.0052	2.203	0.0622	1.778	0.0763	1.867	
81665	0.1768	0.0016	2.114	0.0184	1.859	0.0205	1.895	
326145	0.0884	0.0004	2.054	0.0051	1.949	0.0053	1.936	
1303553	0.0442	0.0001	2.003	0.0014	1.984	0.0016	1.979	
$e(\varphi)$	$r(\varphi)$	$e(\tilde{\mathbf{t}})$	$r(\tilde{\mathbf{t}})$	$e(\tilde{\boldsymbol{\sigma}})$	$r(\tilde{\boldsymbol{\sigma}})$	$e(p)$	$r(p)$	It.
0.0769	–	0.5343	–	0.7424	–	0.1795	–	4
0.0158	2.278	0.1681	1.668	0.2094	1.826	0.0469	1.934	4
0.0033	2.247	0.0474	1.827	0.0576	1.868	0.0097	2.267	4
0.0007	2.126	0.0127	1.898	0.0151	1.925	0.0021	2.185	4
0.0004	2.048	0.0033	1.938	0.0038	1.965	0.0005	2.081	4
0.0001	2.002	0.0009	1.966	0.0013	1.993	0.0001	2.031	4

TABLE 7.1. Example 1: Convergence history and Newton iteration count for the fully-mixed $\mathbf{P}_1 - \mathbb{P}_1 - \mathbb{RT}_1 - \mathbf{P}_1 - \mathbb{P}_1 - \mathbb{RT}_1$ approximation. DoF stands for the number of degrees of freedom associated with each barycentric refined mesh \mathcal{T}_h^b .

Example 1: Convergence against smooth exact solutions

In our first example we study the accuracy of the approximations by manufacturing an exact solution of (3.6) in the domain $\Omega := (-1, 1)^2$ with the constant and variable coefficients

$$\begin{aligned} \mu(\boldsymbol{\varphi}) &= e^{-\varphi_1}, \quad \boldsymbol{\vartheta} = (1, 0.5)^\dagger, \quad \gamma = 10^{-3}, \quad \mathbb{K}_1(\mathbf{x}) = \begin{pmatrix} \exp(-x_1) & x_1/10 \\ x_2/10 & \exp(-x_2) \end{pmatrix}, \\ \mathbb{K}_2(\mathbf{x}) &= \begin{pmatrix} \exp(-x_1) & 0 \\ 0 & \exp(-x_2) \end{pmatrix}, \quad \text{and} \quad \mathbf{g}(\mathbf{x}) = (0, -1)^\dagger \quad \forall \mathbf{x} := (x_1, x_2)^\dagger \in \Omega. \end{aligned}$$

Then, the Dirichlet data \mathbf{u}_D and $\boldsymbol{\varphi}_D$, and the terms on the right-hand sides, are imposed according to the exact solutions given by the smooth functions

$$\begin{aligned} \mathbf{u}(\mathbf{x}) &= \begin{pmatrix} \cos(\frac{\pi}{2}x_1) \sin(\frac{\pi}{2}x_2) \\ -\sin(\frac{\pi}{2}x_1) \cos(\frac{\pi}{2}x_2) \end{pmatrix}, \quad p(\mathbf{x}) = (x_1 - 0.5)(x_2 - 0.5) - 0.25, \\ \varphi_1(\mathbf{x}) &= \exp(-x_1^2 - x_2^2) - \frac{1}{2}, \quad \text{and} \quad \varphi_2(\mathbf{x}) = \exp(-x_1x_2[x_1 - 1][x_2 - 1]) \quad \forall \mathbf{x} := (x_1, x_2)^\dagger \in \Omega. \end{aligned}$$

Values of errors and corresponding convergence rates associated with the approximations with the finite element family $\mathbf{P}_1 - \mathbb{P}_1 - \mathbb{RT}_1 - \mathbf{P}_1 - \mathbb{P}_1 - \mathbb{RT}_1$ are summarized in Table 7.1. As expected, we observe there that the convergence rates are quadratic with respect to h for all the unknowns in their respective norms. Sample solutions of approximate velocity magnitude, temperature, concentration, and postprocessed pressure computed with our fully-mixed method are depicted in Figure 7.2.

Example 2: Manufactured solutions using cross-diffusion

We now perform an accuracy test for (3.48) on the tombstone-shaped domain (see [17])

$$\Omega := \{\mathbf{x} : -0.5 < x_1 < 0.5, -0.5 < x_2 < 0.5\} \cup \{\mathbf{x} : -0.5 < x_1 < 0.5, 0.5 < x_2 < \sin(\pi x_2)\},$$

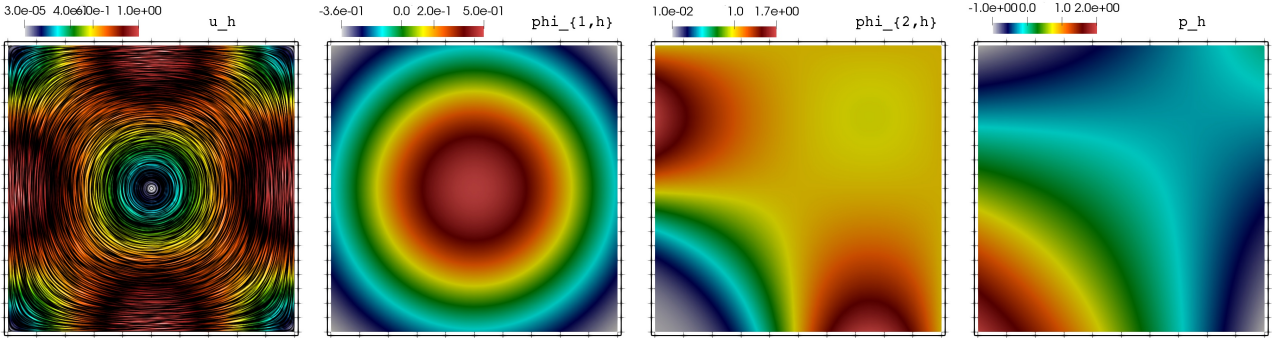


FIGURE 7.2. Example 1: Approximate velocity magnitude, temperature, concentration, and postprocessed pressure, obtained using $k = 1$ and a barycentrically refined mesh with 19110 elements.

and consider the same specification as in Example 1 for viscosity and gravity, while the temperature and concentration now use cross-diffusion effects encoded in the tensor (3.46)

$$\mathbb{K} = \begin{pmatrix} K_{11} & K_{12} \\ K_{21} & K_{22} \end{pmatrix},$$

with $K_{11} = 1, K_{12} = 0.5, K_{2,1} = 0.3, K_{2,2} = 2 + \sin(\pi x_1 x_2)$, and the thermal and mass expansions and inverse permeability are also modified with respect to the previous test

$$\boldsymbol{\vartheta} = (0.75, 0.25)^{\text{t}}, \quad \gamma = 1.0678 \cdot 10^4.$$

Again, the right-hand sides and the boundary Dirichlet data are adjusted in terms of the manufactured exact solutions, which are in this case

$$\mathbf{u}(\mathbf{x}) = \begin{pmatrix} 2\pi \cos(\pi x_2) \sin^2(\pi x_1) \sin(\pi x_2) \\ -2\pi \cos(\pi x_1) \sin(\pi x_1) \sin^2(\pi x_2) \end{pmatrix}, \quad p(\mathbf{x}) = 5x_1 \sin(x_2),$$

$$\varphi_1(\mathbf{x}) = \exp(-x^2 - y^2) - \frac{1}{2}, \quad \text{and} \quad \varphi_2(\mathbf{x}) = 15 - 15 \exp(-x_1 x_2 [x_1 - 1][x_2 - 1]) \quad \forall \mathbf{x} := (x_1, x_2)^{\text{t}} \in \Omega.$$

In Table 7.2 we present errors for each variable with respect to DoF, the experimental convergence rates, and the number of Newton iterations per mesh refinement. This time the computations were done with the finite element family $\mathbf{P}_2 - \mathbb{P}_2 - \mathbb{RT}_2 - \mathbf{P}_2 - \mathbf{P}_2 - \mathbf{RT}_2$ ($k = 2$). In concordance with the theoretical estimates from Section 5, the computational results confirm an error decay with rate $O(h^3)$. A total of 5 Newton iterations were required to reach a tolerance $\text{tol} = 1\text{e-}08$. In Figure 7.3 we display the velocity magnitude, the temperature, and the concentration produced with our fully-mixed scheme on a barycentric refined mesh that, for $k = 2$, generates 633555 DoFs.

Example 3: A posteriori error estimation and adaptive mesh refinement

Next we test the properties of the residual-based a posteriori error estimator (6.4) by considering an L-shaped domain $\Omega = (-1, 1)^2 \setminus (0, 1)^2$, using the same constitutive relations and exact velocity taken in Example 1 above, while we use the following exact pressure and concentration fields having step derivatives towards the reentrant corner

$$p = \frac{2 + \sin(x_1 x_2)}{(x_1 - a)^2 + (x_2 - b)^2}, \quad \varphi_2 = \exp(-100(x_1 - a)^2 - 100(x_2 - b)^2),$$

Finite Element Family: $\mathbf{P}_2 - \mathbb{P}_2 - \mathbb{RT}_2 - \mathbb{P}_2 - \mathbb{P}_2 - \mathbf{RT}_2$								
DoF	h	$e(\mathbf{u})$	$r(\mathbf{u})$	$e(\mathbf{t})$	$r(\mathbf{t})$	$e(\boldsymbol{\sigma})$	$r(\boldsymbol{\sigma})$	
2421	0.7224	0.1468	–	2.0740	–	6.0911	–	
10089	0.4234	2.69e-02	2.763	0.45071	2.683	1.0707	2.178	
39258	0.2460	2.99e-03	3.106	7.10e-02	2.718	0.1624	2.775	
158652	0.1397	3.78e-04	2.963	1.06e-02	2.753	2.56e-02	2.859	
633555	0.0763	5.18e-05	2.906	1.69e-03	2.956	3.43e-03	2.938	
$e(\varphi)$	$r(\varphi)$	$e(\tilde{\mathbf{t}})$	$r(\tilde{\mathbf{t}})$	$e(\tilde{\boldsymbol{\sigma}})$	$r(\tilde{\boldsymbol{\sigma}})$	$e(p)$	$r(p)$	It.
1.82e-02	–	0.4513	–	0.8263	–	5.3892	–	5
2.65e-03	2.7217	6.80e-02	2.634	0.1247	2.724	0.5072	3.026	5
2.15e-04	3.1620	8.79e-03	2.906	1.43e-02	2.892	7.39e-02	2.908	5
2.84e-05	2.9112	1.42e-03	2.924	2.11e-03	2.930	6.89e-03	2.935	5
3.79e-06	2.9606	1.88e-04	2.951	2.80e-04	2.984	9.75e-03	2.998	5

TABLE 7.2. Example 2: Convergence history and Newton iteration count for the fully-mixed $\mathbf{P}_2 - \mathbb{P}_2 - \mathbb{RT}_2 - \mathbb{P}_2 - \mathbb{P}_2 - \mathbf{RT}_2$ approximation of the Oberbeck–Boussinesq equations on a tombstone-shaped domain and using cross-diffusion.

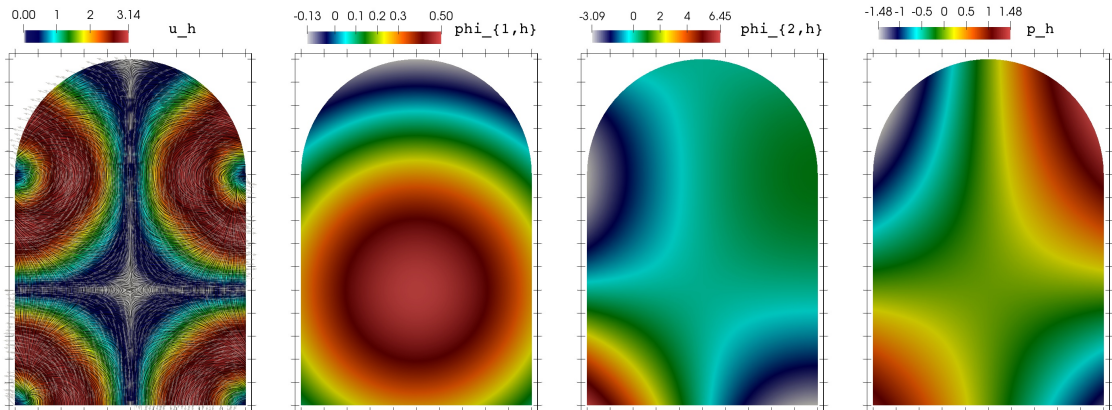


FIGURE 7.3. Example 2: Approximate velocity magnitude, temperature, concentration, and postprocessed pressure, using $k = 2$ and a barycentric refinement with 11534 triangular elements.

with $a = b = 0.01$. The values of the exact solutions are used for boundary conditions. Obtaining optimal rates of convergence depends on having sufficient regularity of the exact solution, which is not the case here. The local contributions of the residual-based a posteriori error estimator (6.4) are used to steer the adaptive mesh-refining algorithm outlined in Section 6.3.

The error history for each field variable and the effectivity index $\text{eff}(\Psi) := \mathbf{e}/\Psi$ (where \mathbf{e} denotes the total error) are plotted in the top panels of Figure 7.4. We compare the convergence of the method when following a uniform mesh refinement versus the adaptive case. In all cases we see that the convergence is suboptimal for the uniform refinement whereas rates much closer to the optimal $O(h^2)$ are generated by the adaptive algorithm. Also, the effectivity index remains stable in the adaptive case, while it shows large oscillations in the uniform case. In the second row of the same figure we show examples of locally refined meshes that indicate that additional refinement is effectuated towards the

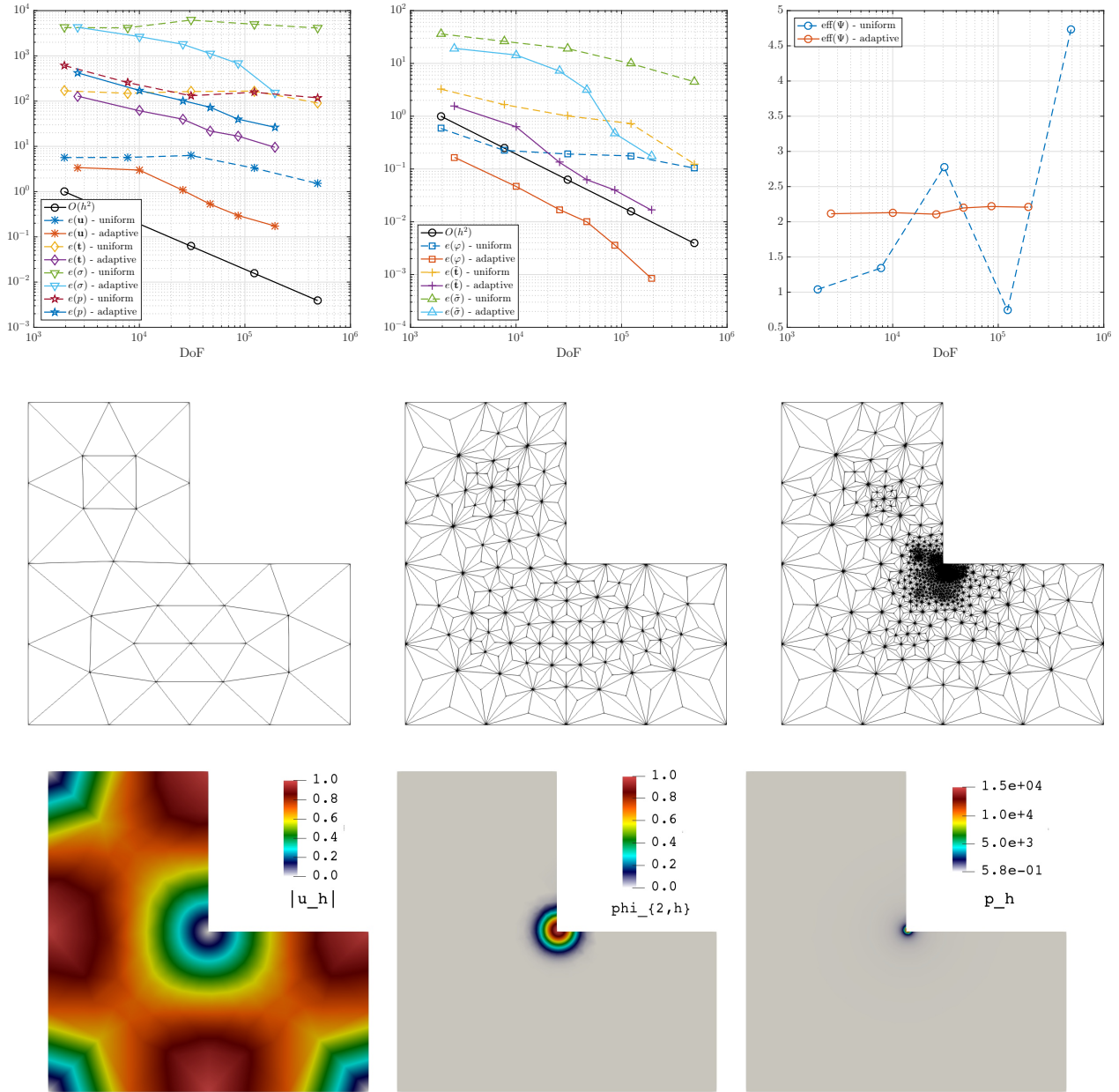


FIGURE 7.4. Example 3. Top: Error history and effectivity index for the fully-mixed method on a non-convex domain using exact solutions with high gradients and uniform vs. adaptive mesh refinement. Middle row: Initial triangulation (left) and samples of intermediate barycentric refinements obtained after three (center) and five (right) steps of mesh adaptation according to the a posteriori error estimator (6.4). Bottom panels: samples of approximate solutions on coarse adapted meshes.

reentrant corner. We also show examples of approximate solutions obtained by the adaptive method on relatively coarse meshes.

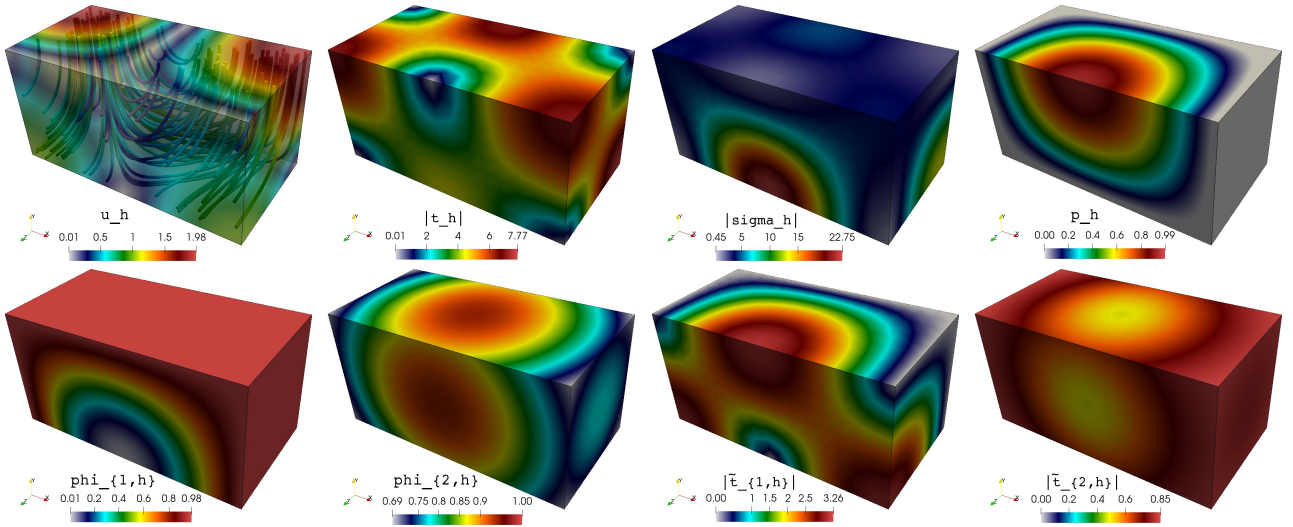


FIGURE 7.5. Example 4: Approximate velocity magnitude and streamlines, velocity gradient, Bernoulli tensor, postprocessed pressure, temperature, concentration, temperature gradient, and concentration gradient, obtained using $k = 2$ and a barycentrically refined tetrahedral mesh with 24576 elements.

Example 4: Error decay in the 3D case

Verification of the convergence of the method in 3D is provided with a simple test employing the following closed-form solutions

$$\mathbf{u}(\mathbf{x}) = \begin{pmatrix} \sin(\pi x_1) \cos(\pi x_2) \cos(\pi x_3) \\ -2 \cos(\pi x_1) \sin(\pi x_2) \cos(\pi x_3) \\ \cos(\pi x_1) \cos(\pi x_2) \sin(\pi x_3) \end{pmatrix}, \quad p(\mathbf{x}) = \sin(\pi x_1) \sin(\pi x_2) \sin(\pi x_3),$$

$$\varphi_1(\mathbf{x}) = 1 - \sin(\pi x_1) \cos(\pi x_2) \sin(\pi x_3), \quad \varphi_2(\mathbf{x}) = \exp(-(x_1 - 0.5)^2 - (x_2 - 0.25)^2 - (x_3 - 0.25)^2),$$

for $\mathbf{x} := (x_1, x_2, x_3)^\top \in \Omega$. The manufactured velocity is divergence-free and we use it to impose the Dirichlet condition on Γ . The exact concentration and temperature are uniformly bounded in Ω and we consider the following constant and variable coefficients

$$\gamma = 1, \quad \boldsymbol{\vartheta} = (1, 0.5)^\top, \quad \mathbb{K}_1(\mathbf{x}) = \begin{pmatrix} \exp(-x_1) & 0 & 0 \\ 0 & \exp(-x_2) & 0 \\ 0 & 0 & \exp(-x_3) \end{pmatrix}, \quad \mathbb{K}_2 = \mathbb{I},$$

We recall that the solvability of the discrete problem requires that, for dimension $n = 3$, the finite element spaces made precise in (4.21)–(4.26) should use a polynomial degree $k \geq 2$. The error history is shown in Table 7.3, where the tabulated convergence rates with respect to DoF indicate that all individual fields have optimal error decay as predicted by (5.9). In all cases the number of Newton iterations needed to reach convergence was 4. The solutions on a coarse mesh with 7521 vertices and 24576 tetrahedral elements (actually representing 957121 DoFs for $k = 2$), are displayed in Figure 7.5.

Example 5: Simulating exothermic flows

We finalize with a time-dependent problem that has relevance in the modeling of exothermic reaction-diffusion fronts in porous media. The problem configuration is adapted from that in [39], where apart

Finite Element Family: $\mathbf{P}_2 - \mathbb{P}_2 - \mathbb{RT}_2 - \mathbf{P}_2 - \mathbf{P}_2 - \mathbf{RT}_2$								
DoF	h	$e(\mathbf{u})$	$r(\mathbf{u})$	$e(\mathbf{t})$	$r(\mathbf{t})$	$e(\boldsymbol{\sigma})$	$r(\boldsymbol{\sigma})$	
7621	1.225	0.03165	–	0.55572	–	2.4535	–	
15181	0.866	0.01095	3.063	0.18479	3.178	0.8475	3.066	
120241	0.433	0.00143	2.935	0.02785	2.829	0.1554	2.773	
957121	0.2165	0.00026	2.893	0.00484	2.881	0.0293	2.835	
7965323	0.1083	0.00007	2.970	0.00063	2.992	0.0046	2.916	
$e(\varphi)$	$r(\varphi)$	$e(\tilde{\mathbf{t}})$	$r(\tilde{\mathbf{t}})$	$e(\tilde{\boldsymbol{\sigma}})$	$r(\tilde{\boldsymbol{\sigma}})$	$e(p)$	$r(p)$	It.
0.01043	–	0.10795	–	0.22103	–	0.23510	–	4
0.00397	2.766	0.03389	3.305	0.06753	3.421	0.03295	2.895	4
0.00049	3.029	0.00518	2.705	0.00932	2.860	0.00464	2.974	4
5.99e-05	3.032	0.00069	2.814	0.00120	2.897	0.00087	3.012	4
7.45e-06	2.989	8.17e-05	2.909	1.62e-04	2.936	1.13e-04	3.003	4

TABLE 7.3. Example 4: Convergence history and Newton iteration count for the fully-mixed $\mathbf{P}_2 - \mathbb{P}_2 - \mathbb{RT}_2 - \mathbf{P}_2 - \mathbb{P}_2 - \mathbf{RT}_2$ approximation of the Oberbeck–Boussinesq equations on a 3D box.

from advection and diffusion, a reaction term is present in the right-hand sides of the temperature and concentration equation. More precisely, they are $\text{Da}f(\varphi_2)$ in the equation for φ_1 and $-\text{Da}f(\varphi_2)$ in the equation for φ_2 , where $\text{Da} = 0.001$ is the dimensionless Darcy number and the concentration-dependent nonlinear reaction is $f(\varphi_2) := \varphi_2(1 + 7\varphi_2)(1 - \varphi_2)^2$. The buoyancy term is characterized by $\boldsymbol{\vartheta} = (5, -1)^\top$, and we simply consider a constant viscosity $\mu = 1$ and a constant permeability $\gamma = 1$. The diffusivities are isotropic and constant $\mathbb{K}_1 = 8\mathbb{I}$, $\mathbb{K}_2 = 2.5\mathbb{I}$, and the domain is the rectangle $\Omega = (0, 2000) \times (-1000, 0)$. Further differences with respect to the original system (2.1) include boundary conditions: we now set $\mathbf{u}_D = \mathbf{0}$ on the whole boundary whereas we put $\varphi_j = 1$ on the top edge of the domain, $\varphi_j = 0$ on the bottom surface, and on the vertical walls we impose zero flux conditions, which in the context of our mixed formulation are implemented as essential conditions for each $\tilde{\mathbf{t}}_j$. A barycentric refinement is applied on an unstructured triangulation of the domain and the resulting grid has 32491 elements. In the bilinear forms $\tilde{\mathcal{A}}_{\mathbf{u},j}$ we add the term

$$\int_{\Omega} \frac{1}{\Delta t} (\varphi_j^{\ell+1} - \varphi_\ell) \psi_j,$$

accounting for the backward Euler time discretization of $\partial_t \varphi_j$, $j \in \{1, 2\}$. The same is done to add an acceleration term to the momentum equation. We use a uniform partition of the time domain (from 0 to 2000) and use a constant stepsize of $\Delta t = 20$. The fully mixed scheme is defined by (4.21)–(4.26) with $k = 1$, and the initial conditions for the solutal concentration and high temperature near the domain top surface are uniformly distributed random perturbations, whereas the initial velocity is the zero vector.

We run the system until 2000 time units and show in Figure 7.6 snapshots of concentration of the solute at three different times, together with the postprocessed pressure. As a result of the nonlinear interaction between the change of temperature and the high solute concentration, density-driven instabilities start to form and the solute fingers commence to move downwards also due to gravitational effects. Throughout the computation the Newton–Raphson method took at most five iterations to reach the desired tolerance.

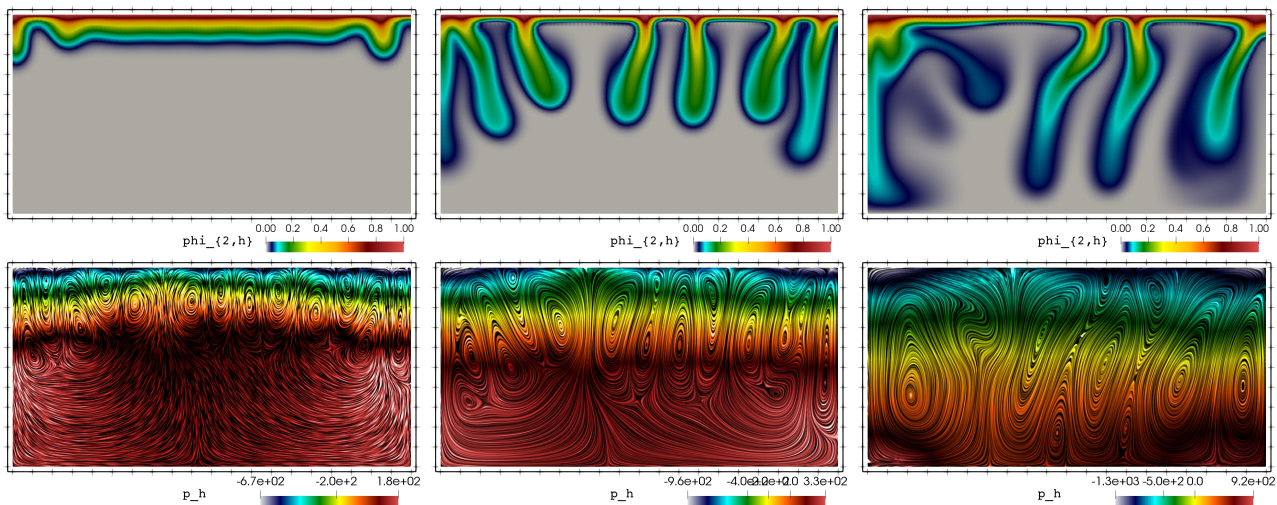


FIGURE 7.6. Example 4: Evolution of the solute concentration (top) and the post-processed pressure (bottom, showing also line integral contours of velocity) computed with a method using $k = 1$, and recorded at adimensional time instants 800 (left), 1200 (center), and 2000 (right panels).

References

- [1] Bushra Al-Sulaimi. The non-linear energy stability of Brinkman thermosolutal convection with reaction. *Ric. di Mat.*, 65(2):381–397, 2016.
- [2] Gennady Alekseev, Dmitry Tereshko, and Vladislav Pukhnachev. Boundary Control Problems for Oberbeck–Boussinesq Model of Heat and Mass Transfer. In *Advanced Topics in Mass Transfer*, pages 485–512. IntechOpen, 2011.
- [3] H. Alhumade and J. Azaiez. Reversible reactive flow displacements in homogeneous porous media. In *Proceedings of the World Congress on Engineering 2013 Vol III*, pages 1681–1686, 2013.
- [4] S. Aliabadi, A. Johnson, J. Abedi, S. Tu, and A. Tate. Simulation of contaminant dispersion on the cray X1: Verification and implementation. *J. Aerosp. Comput. Inf. Commun.*, 8:341–361, 2004.
- [5] Karam Allali. A priori and a posteriori error estimates for Boussinesq equations. *Int. J. Numer. Anal. Model.*, 2(2):179–196, 2005.
- [6] Javier A. Almonacid and Gabriel N. Gatica. A fully-mixed finite element method for the n -dimensional Boussinesq problem with temperature-dependent parameters. *Comput. Methods Appl. Math.*, 20(2):187–213, 2020.
- [7] Javier A. Almonacid, Gabriel N. Gatica, Ricardo Oyarzúa, and Ricardo Ruiz-Baier. A new mixed finite element method for the n -dimensional Boussinesq problem with temperature-dependent viscosity. *Netw. Heterog. Media*, 15(2):215–245, 2020.
- [8] M. S. Alnæs, J. Blechta, J. Hake, A. Johansson, B. Kehlet, A. Logg, C. Richardson, J. Ring, M. E. Rognes, and G. N. Wells. The FEniCS Project Version 1.5. *Arch. Numer. Softw.*, 3(100):9–23, 2015.
- [9] Mario Alvarez, Gabriel N. Gatica, Bryan Gomez-Vargas, and Ricardo Ruiz-Baier. New mixed finite element methods for natural convection with phase-change in porous media. *J. Sci. Comput.*, 80(1):141–174, 2019.
- [10] Mario Alvarez, Gabriel N. Gatica, and Ricardo Ruiz-Baier. An augmented mixed-primal finite element method for a coupled flow-transport problem. *ESAIM, Math. Model. Numer. Anal.*, 49(5):1399–1427, 2015.

- [11] Christine Bernardi, Brigitte Métivet, and Bernadette Pernaud-Thomas. Couplage des équations de Navier-Stokes et de la chaleur : le modèle et son approximation par éléments finis. *ESAIM, Math. Model. Numer. Anal.*, 29(7):871–921, 1995.
- [12] Daniele Boffi, Franco Brezzi, and Michel Fortin. Reduced symmetry elements in linear elasticity. *Commun. Pure Appl. Anal.*, 8(1):95–121, 2009.
- [13] Daniele Boffi, Franco Brezzi, and Michel Fortin. *Mixed Finite Element Methods and Applications*, volume 1. Springer, 2013.
- [14] J. Boland and W. Layton. An analysis of the finite element method for natural convection problems. *Numer. Methods Partial Differ. Equ.*, 6(2):115–126, 1990.
- [15] Franco Brezzi and Michel Fortin. *Mixed and Hybrid Finite Element Methods*. Springer, 1991.
- [16] Raimund Bürger, Paul E. Mendez, and Ricardo Ruiz-Baier. On $H(\text{div})$ -conforming methods for double-diffusion equations in porous media. *SIAM J. Numer. Anal.*, 57(3):1318–1343, 2019.
- [17] Jessika Camaño, Gabriel N. Gatica, Ricardo Oyarzúa, Ricardo Ruiz-Baier, and Pablo Venegas. New fully-mixed finite element methods for the Stokes-Darcy coupling. *Comput. Methods Appl. Mech. Eng.*, 295:362–395, 2015.
- [18] Sergio Caucao, Gabriel N. Gatica, and Ricardo Oyarzúa. A posteriori error analysis of a fully-mixed formulation for the Navier–Stokes/Darcy coupled problem with nonlinear viscosity. *Comput. Methods Appl. Mech. Eng.*, 315:943–971, 2017.
- [19] Ping Cheng. Heat Transfer in Geothermal Systems. *Adv. Heat Transf.*, 14(C):1–105, 1979.
- [20] Philippe G. Ciarlet. *Linear and Nonlinear Functional Analysis with Applications*. Society for Industrial and Applied Mathematics, 2013.
- [21] Aytekin Çibik and Songül Kaya. Finite element analysis of a projection-based stabilization method for the Darcy-Brinkman equations in double-diffusive convection. *Appl. Numer. Math.*, 64:35–49, 2013.
- [22] Eligio Colmenares, Gabriel N. Gatica, and Sebastian Moraga. A Banach spaces-based analysis of a new fully-mixed finite element method for the Boussinesq problem. *ESAIM, Math. Model. Numer. Anal.*, 2020.
- [23] Eligio Colmenares, Gabriel N. Gatica, and Ricardo Oyarzúa. An augmented fully-mixed finite element method for the stationary Boussinesq problem. *Calcolo*, 54(1):167–205, 2017.
- [24] Eligio Colmenares and Michael Neilan. Dual-mixed finite element methods for the stationary Boussinesq problem. *Comput. Math. Appl.*, 72(7):1828–1850, 2016.
- [25] Helene Dallmann and Daniel Arndt. Stabilized finite element methods for the Oberbeck–Boussinesq model. *J. Sci. Comput.*, 69(1):244–273, 2016.
- [26] Willy Dörfler. A convergent adaptive algorithm for Poisson’s equation. *SIAM J. Numer. Anal.*, 33(3):1106–1124, 1996.
- [27] A. Ern and J.-L. Guermond. *Theory and Practice of Finite Elements*, volume 159 of *Applied Mathematical Sciences*. Springer, 2004.
- [28] M. Farhloul, S. Nicaise, and L. Paquet. A mixed formulation of Boussinesq equations: Analysis of nonsingular solutions. *Math. Comput.*, 69(231):965–987, 2000.
- [29] M. Farhloul, S. Nicaise, and L. Paquet. A refined mixed finite element method for the Boussinesq equations in polygonal domains. *IMA J. Numer. Anal.*, 21(2):525–551, 2001.
- [30] Gabriel N. Gatica. *A Simple Introduction to the Mixed Finite Element Method*. Springer, 2014.
- [31] Gabriel N. Gatica, Cristián Inzunza, Ricardo Ruiz-Baier, and Felipe Sandoval. A posteriori error analysis of Banach spaces-based fully-mixed finite element methods for the Boussinesq and related models. in preparation.
- [32] B. Gebhart and L. Pera. The nature of vertical natural convection flows resulting from the combined buoyancy effects of thermal and mass diffusion. *Int. J. Heat Mass Transf.*, 14(12):2025–2050, 1971.

- [33] Christophe Geuzaine and Jean François J.-F. Remacle. Gmsh: A 3-D finite element mesh generator with built-in pre- and post-processing facilities. *Int. J. Numer. Methods Eng.*, 79(11):1309–1331, 2009.
- [34] Moez Hammami, Mohamed Mseddi, and Mounir Baccar. Numerical study of coupled heat and mass transfer in a trapezoidal cavity. *Eng. Appl. Comput. Fluid Mech.*, 1(3):216–226, 2007.
- [35] Jason S. Howell and Noel J. Walkington. Inf-sup conditions for twofold saddle point problems. *Numer. Math.*, 118(4):663–693, 2011.
- [36] Pengzhan Huang, Wenqiang Li, and Zhiyong Si. Several iterative schemes for the stationary natural convection equations at different Rayleigh numbers. *Numer. Methods Partial Differ. Equ.*, 31(3):761–776, 2015.
- [37] Mamoru Ishii and Takashi Hibiki. *Thermo-fluid dynamics of two-phase flow*. Springer, 2006.
- [38] Mohammad Karimi-Fard, M. C. Charrier-Mojtabi, and K. Vafai. Non-darcian effects on double-diffusive convection within a porous medium. *Numer. Heat Transf. Part A Appl.*, 31(8):837–852, 1997.
- [39] Pietro Lenarda, Marco Paggi, and Ricardo Ruiz Baier. Partitioned coupling of advection–diffusion–reaction systems and Brinkman flows. *J. Comput. Phys.*, 344:281–302, 2017.
- [40] Donald A. Nield and Adrian Bejan. *Convection in Porous Media*. Springer, 2017.
- [41] Ricardo Oyarzúa and Paulo Zúñiga. Analysis of a conforming finite element method for the Boussinesq problem with temperature-dependent parameters. *J. Comput. Appl. Math.*, 323:71–94, 2017.
- [42] L. Pera and B. Gebhart. Natural convection flows adjacent to horizontal surfaces resulting from the combined buoyancy effects of thermal and mass diffusion. *Int. J. Heat Mass Transf.*, 15(2):269–278, 1972.
- [43] Alfio Quarteroni and Alberto Valli. *Numerical Approximation of Partial Differential Equations (Springer Series in Computational Mathematics)*, volume 23 of *Springer Series in Computational Mathematics*. Springer, 1996.
- [44] S. C. Saha and M. A. Hossain. Natural convection flow with combined buoyancy effects due to thermal and mass diffusion in a thermally stratified media. *Nonlinear Anal. Model. Control*, 9(1):89–102, 2004.
- [45] L. R. Scott and Michael Vogelius. Conforming finite element methods for incompressible and nearly incompressible continua. *NASA STI/Recon Tech. Rep. N.*, 22:221–244, 1984.
- [46] Masahisa Tabata and Daisuke Tagami. Error estimates of finite element methods for nonstationary thermal convection problems with temperature-dependent coefficients. *Numer. Math.*, 100(2):351–372, 2005.
- [47] Rüdiger Verfürth. *A Posteriori Error Estimation Techniques for Finite Element Methods*. Oxford University Press, 2013.
- [48] James Woodfield, Mario Alvarez, Bryan Gómez-Vargas, and Ricardo Ruiz-Baier. Stability and finite element approximation of phase change models for natural convection in porous media. *J. Comput. Appl. Math.*, 360:117–137, 2019.